BAF155 regulates the genesis of basal progenitors through both Pax6-dependent and independent mechanisms during cerebral cortex development

Dissertation

for the award of the degree

"Doctor rerum naturalium"

Faculty of Biology

of the Georg-August-Universität Göttingen

within the doctoral program

International Max Planck Research School for Neurosciences

of the Georg-August University School of Science (GAUSS)

submitted by

Ramanathan Narayanan

Born in Puducherry, India

Göttingen 2017

Thesis Committee

Prof. Dr. Jochen F. Staiger, Institute of Neuroanatomy, University Medical Centre, Goettingen

Prof. Andre Fischer, German Centre for Neurodegenerative diseases (DZNE), Goettingen

Prof. Klaus-Armin Nave, Max Planck Institute for Experimental Medicine, Goettingen

Members of the Examination Board

First Referee:

Prof. Dr. Jochen F. Staiger, Institute of Neuroanatomy, University Medical Centre, Goettingen

Second Referee:

Prof. Andre Fischer, German Centre for Neurodegenerative diseases (DZNE), Goettingen

Further members of the Examination Board

Prof. Klaus-Armin Nave, Max Planck Institute for Experimental Medicine, Goettingen

Prof. Anastassia Stoykova, Max Planck Institute for Biophysical Chemistry, Goettingen

Prof. Gregor Eichele, Max Planck Institute for Biophysical Chemistry, Goettingen

Prof. Ahmed Mansouri, Max Planck Institute for Biophysical Chemistry, Goettingen

Date of the oral examination: 28.07.2017

I, Ramanathan Narayanan, hereby certify that the present doctoral thesis has been written independently with no other sources than cited. All results presented here were the outcome of my own workings unless stated otherwise.

.....

Göttingen, 08.06.2017

Table of Contents

Table of Figures

Introduction

The mammalian cerebral cortex is a sheet of cells covering the cerebrum that provides the structural basis for perception of sensory inputs, motor output responses, cognitive function, and the mental capacity of higher primates. The development of the cortex is a tightly regulated process that involves expansion of the neural progenitor pool and waves of asymmetric division to generate an array of specialized neuronal subtypes that comprise the six layers of the cortex (Gotz and Huttner, 2005; Kriegstein et al., 2006; Leone et al., 2008; Molyneaux et al., 2007; O'Leary et al., 2007). Before the onset of neurogenesis, neuroepithelial cells divide mostly in a symmetric manner leading to exponential progenitor production and tangential growth of the cortex. During neurogenesis, neuroepithelial cells acquire distinct characteristics to become radial glial cells (RGs) that populate the ventricular zone (VZ), which is not only a scaffold for neuronal migration (Gadisseux et al., 1990; Hatten and Mason, 1990; Rakic, 1972) but also a precursor for most cortical cell types (Choi and Lapham, 1978; Levitt et al., 1983; Malatesta et al., 2000; Misson et al., 1991). In addition to self-renewal, through asymmetric cell divisions RGs produces either one neuron or a neurogenic intermediate progenitor (IP) that populate the basally located sub-ventricular zone (SVZ) (Miyata, 2007). IPs are transit-amplifying cells which increases neuronal output by undergoing terminal differentiation (Haubensak et al., 2004; Miyata et al., 2004; Noctor et al., 2004; Pontious et al., 2008). Thus, symmetric cell divisions regulate the tangential size of the cerebral cortex, whereas asymmetric cell divisions lead to radial growth of the cerebral cortex and the balance between them is critical in defining a proper size and shape of cerebral cortex (Farkas and Huttner, 2008; Rakic, 2009).

During mammalian evolution, the size and shape of the cerebral cortex has greatly diversified, for instance, ranging from a smooth lissencephalic rodent cortex to folded gyrencephalic primate cortex. In an attempt to understand the features that make a gyrencephalic cortex distinct, few seminal studies in both primate and human tissues, identified a novel basal progenitor cell type, termed as outer or basal radial glial cells (bRGs) (Betizeau et al., 2013; Fietz et al., 2010; Hansen et al., 2010) which are much less abundant in rodent cortex (Wang et al., 2011). The bRGs share several characteristics with the ventricular RGs (vRGs), however lacking apical contact and having a distinct pia-directed process. Collectively, the basal progenitors (BPs) - bRGs together with basal intermediate progenitors (bIPs), form a distinct zone termed as outer sub-ventricular zone (oSVZ), which is basally located to inner SVZ (iSVZ; identical to rodent SVZ) in primate and human cortex (Hansen et al., 2010; Wang et al., 2011). Interestingly, the appearance of oSVZ during cortical development is found to be

tightly associated with increased neuronal output, cortical expansion and folding (Dehay and Kennedy, 2007; Lui et al., 2011).

Although there are species-specific differences in cortical cell types, there is a unifying theme that underlies cortical expansion – genesis of basal progenitors, which results in increased neuronal output compared to apical progenitors. Despite the importance of basal progenitors in mammalian cerebral cortical evolution, we are just beginning to uncover the complex molecular machinery that regulates the genesis of BPs (Fish et al., 2008; Molnar et al., 2006). Studies in the past decade have primarily focused on the role of neurogenic transcription factors (cell-intrinsic) and signalling cascades (cell-extrinsic) in the decision of progenitor cells to either self-renew or differentiate (Gotz and Huttner, 2005; Guillemot, 2007; Kriegstein et al., 2006). The role of epigenetic mechanisms in forebrain development is implicit based in part, on the rising number of neurodevelopmental disorders caused by mutations in genes encoding chromatin remodeling proteins (van Bokhoven and Kramer, 2010). In addition, the use of neural stem cell cultures and mouse models have begun to elucidate the epigenetic mechanisms controlling neurogenesis (Guillemot, 2007; Hsieh and Gage, 2005; Wen et al., 2009). Therefore, deciphering the interplay between neurogenic transcription factors and epigenetic regulators is paramount to our understanding of cerebral cortex development. However, linking chromatin changes to specific pathways that control cortical histogenesis remains a challenge.

In our previous studies, we have elucidated such a link between BAF chromatin remodelling complex and transcriptional programs that regulate cerebral cortical size and thickness. Specifically, we have shown that the BAF170 subunit of BAF complex inhibits IP genesis through downregulation of IP-specific gene expression by recruiting a transcriptional co-repressor and ultimately regulating cortical expansion (Tuoc et al., 2013). In addition, we have also shown that the two core subunits of BAF complex, BAF170 and BAF155 is crucial for the proper development of cerebral cortex by regulating global transcriptional and chromatin state changes (Narayanan et al., 2015).

To gain new insights into the regulation of the mode of cell division and basal progenitor genesis in cortical development, we took a different approach by examining the role of the transcription factor Pax6, a known regulator of corticogenesis and cell division (Estivill-Torrus et al., 2002; Georgala et al., 2011; Gotz et al., 1998; Tuoc et al., 2009) and BAF155 subunit of BAF chromatin remodeling complex, a Pax6-interacting protein. We found BAF155 potentiates Pax6-dependent transcriptional activity, such that the synergistic interaction between BAF155 and Pax6 controls the fate choice of mouse vRGs – by promoting IP genesis and suppressing the genesis of bRGs specifically during early cortical

development. Besides a cell-autonomous role in regulating vRG division, we also found that the loss of BAF155 and Pax6 causes delamination of RGs from the VZ to generate bRGs, at least in part, through a novel CEP4 dependent non-cell autonomous mechanism. Interestingly, our results also suggested that such a non-cell autonomous mechanism of BP genesis might be a hallmark of primate cortical development.

Materials and methods

Mouse husbandry

Husbandry of mice was carried out according to guidelines approved by the University Medical Centre Goettingen and animals were handled in accordance with the German Animal Protection Law. Light/dark cycle in the vivarium was 12 h light on and 12 h light off. Floxed *BAF155* (Choi et al., 2012), floxed *Pax6 (*Ashery-Padan et al., 2000), *Emx1-Cre* (Gorski et al., 2002), *hGFAP-Cre* (Zhuo et al., 2001), and *Nex-Cre* (Goebbels et al., 2006) mice were maintained in a C57BL6/J background. The day of vaginal plug detection was considered embryonic day (E) 0.5.

Genotyping

Genotyping was performed by PCR on tail DNA (embryo) following routine laboratory protocol. Tail biopsies of less than 5mm length were transferred in 0.5ml lysis buffer and incubated rotating for several hours or overnight at 55°C in a modified hybridization oven. Following complete lysis, hairs and tissue residues were removed by centrifugation in an Eppendorf centrifuge at maximal speed (13.1 x 103rpm ~ 16.000 xg) for 10-20 minutes. The supernatant was poured into 0.5ml isopropanol and mixed well. DNA-precipitates were transferred in 300-500µl TE-buffer. To solve the DNA, tubes were again rotated at 55°C for several hours. PCR was carried out using approximately 80ng of genomic DNA (~2µl) and 0.6µM each of the respective primers in a 30µl reaction containing 0.2mM dNTPs, 1.5 U of HotstarTaq-polymerase, 3µl 10xPCRbuffer and 3µl 5xQ-solution. Cycling conditions were: 15-20 minutes at 94°C for HotStarTaq-activation and 10 cycles at 94°C for 30 seconds and a touchdown of 0.5°C each cycle from 55°C at the beginning to 50°C at the 10^{th} cycle for 30 seconds to prevent mis-annealing of primers and therefore to maximize the yield of specific products. Then 35 cycles at 94°C for 30 seconds, at 48°C for 30 seconds and at 72°C for 1 minute followed. Finally, amplicons were extended at 72°C for 10 minutes. 15µl of each PCR-product was analyzed on a 1.8% agarose-TBE-gel.

Tissue preparation for histology

Mouse brains were dissected in cold PBS and fixed in 4% paraformaldehyde (in PBS) for 2 h (embryonic) and overnight (postnatal). After fixation and washing (with PBS), brains were transferred to a 20% (w/v) sucrose solution overnight. Brains were cryoprotected, frozen and embedded in Tissue-Plus (Fisher Scientific), and sectioned (12-14µm) using a cryostat (Leica). Sections were collected in Superfrost®-Plus slides.

Antibodies

The following polyclonal (pAb) and monoclonal (mAb) primary antibodies used in this study were obtained from the indicated commercial sources: Actin-beta (1:500, Sigma), AP2 gamma mouse mAb (1:100; Abcam), BAF155 mouse mAb (1:100; Santa Cruz), BAF170 rabbit pAb (Bethyl), BLBP rabbit pAb (1:200; Chemic), Brn2 goat pAb (1:100; Santa Cruz), Casp-3 rabbit pAb (1:100; Cell Signaling), Ctip2 rat pAb (1:200; Abcam), Flag mAb (1:1000; Sigma), GAPDH rabbit pAb (Santa Cruz), GFP (1:400, Abcam), GLAST pAb pig (1:500; Frontier), Luciferase (1:2000, Abcam), Ngn2 (1:20, Santa Cruz), Pax6 mAb mouse (1:100; Developmental Studies Hybridoma Bank), phospho-H3 rat pAb (1:300; Abcam), pVim mouse mAb (1:500; MBL), Sox2 mouse mAb (1:100; R&D Systems), Tau (1:200, Millipore), Tbr1 rabbit pAb (1:300; Chemicon), Tbr2 rabbit pAb (1:200; Abcam), Tuj mouse mAb (1:500; Chemicon).

Secondary antibodies used were peroxidase-conjugated goat anti-rabbit IgG (1:10000; Covance); peroxidase-conjugated goat anti-mouse IgG (1:5000; Covance); peroxidase-conjugated goat anti-rat IgG (1:10000; Covance); and Alexa 488-, Alexa 568-, Alexa 633- and Alexa 647-conjugated IgG (various species, 1:400; Molecular Probes).

Immunohistochemistry

Cryo-protected sections (12-14 µm thick) of mouse brains were permeabilized with 0.5% Triton X-100 in PBS (PBT), and blocked for 2h at RT with 10% FCS in PBT. Sections were then incubated overnight with the indicated primary antibodies. After washing, the sections were incubated with species-specific secondary antibodies from the Alexa series (Invitrogen) in blocking solution for 2 h at RT and washed again. Cover slips were mounted onto glass slides using Vectashield mounting medium containing DAPI (Vector laboratories). Detailed descriptions were provided previously (Narayanan et al., 2015).

Plasmids

Plasmids used in this study: pCON-P3-Luc (2xP6CON plus 3xP3 sequences in pGL3 basic, Promega as described in Tuoc & Stoykova, 2008); pCIG2-ires-eGFP, pCIG2-Cre-ires-eGFP (gift from Dr. Francois Guillemot, NIMR London); pLuc-Ssx2ip, pLuc-Wnt5a, pLuc-Fgfr1, pLuc-Celsr1, pLuc-Pdgfrb, pLuc-Cdc42ep1 and pLuc-Cdc42ep4 (PCR based amplification of respective gene promoter from genomic DNA followed by cloning into pGL3 basic, Promega); shCEP4 (custom made); pCIG2-CEP4 (CEP4 ORF cDNA cloned into pCIG2-ires-eGFP).

Cell culture

Cell culture medium DMEM+ was prepared by adding 5ml (10%) of heat-inactivated FCS into 45ml DMEM (Cat. 41965-039, Gibco) and 500µl of Pen-Strep (Gibco). Vials containing cells (from liquid N2) were thawed in 37ºC waterbath for 5 min (not longer) and the vial contents were transferred into a falcon tube with 9ml of DMEM (pre-warmed at 37^{o}C). After centrifugation for 6min at 2000 rpm at RT, supernatant was aspirated by glass pipette connected to the vacuum pump (recommended: sterilize glass pipette in the bunsen flame before every use). Then, 10ml of DMEM+ was added and the pellet was thoroughly resuspended by pipetting up and down. The cell suspension is then moved into T75 filter-flasks and incubated at 37ºC. When the cells reached confluence, they were washed with 5-10ml 1xPBS and 5ml Trypsin was added to detach the cells from the floor of the flask. After incubation for 5min at 37ºC, 5ml DMEM was added to stop trypsin activity and the cells were suspended by pipetting up and down. After cell counting in a small volume, the rest were centrifuged at 2000rpm for 6min. After centrifugation, the cells were resuspended in an appropriate volume of medium (e.g. 2x10^{5} cells/ml) and transferred to a 12-well plate (e.g. 1ml of 1x10^{5} cells/well) and culture ON before transfection. Around 1µg DNA was prepared in about 1-5µl endotoxin-free TE followed by addition of 200µl of Opti-MEM I Reduced Serum Medium (Gibco) and mixed gently. The mixture was kept at RT for 5 min and 5µl Lipofectamine 2000 (Life Technologies) was added into the mixture and mixed thoroughly and vigorously. After leaving the mixture to stand at RT for 20min, it was spinned down shortly and added to each well of a 12-well plate containing cells. The cells were then incubated at 37ºC in the CO2 incubator for 24-48h (with occasional change of medium) until they are ready for transgene expression assay.

Protein extraction and western blotting

The medium was removed from the wells, washed with PBS, 0.3 ml Trypsin (per well of 12-well plate) was added and incubated for 5min at 37ºC. The plate was rocked to detach the cells. Then, 0.3 – 0.6 ml DMEM medium was added and the cells were collected in a 1.5ml tube. The tubes were then centrifuged at 2000 rpm for 5min. Without vortexing, PBS was added to wash the cells, centrifuged again at 2000 rpm for 5min. Then, 50-100µl of 2x Sample buffer + 5% of 2-Mercaptoethanol were added, vortexed vigorously and heated at 95-100ºC for 3-5 min. The protein concentration was quantified using Nanodrop (Thermo Scientific; A280 measurement). Samples were then stored at -20ºC and before using for western blot centrifuged at a full speed (13,000 rpm) for 2 min.

For protein separation, 10µl of respective protein samples were loaded onto a SDS-polyacrylamide gel (resolving gel: 10%; stacking gel: 4%, 8 cm x 10 cm x 1.5 mm). Gel was run in SDS-page running buffer

with constant 110V for about 1 hour. Proteins were transferred to nitrocellulose by semidry-blotting: Polyvinylidene fluoride (PVDF) membranes were pre-treated with 100%MeOH for 20 seconds, washed for 10 minutes in H_20 and stored in semidry-blotting buffer. Electrotransfer of proteins to PVDF-membranes took about 2-3 hours at 0.8mA per cm^2. After protein transfer membranes were washed in TBS for 5 minutes at RT and were blocked for 1 hour in skimmed milk blocking buffer followed by three consecutive washing steps in TBS/T for 5 minutes at RT. Membranes were incubated in primary antibody diluted in skimmed milk blocking buffer with gentle agitation overnight at 4°C. After washing the membrane in TBS/T three times for 5 minutes, the membrane was incubated in HRP-conjugated secondary antibody with gentle agitation for 1 hour at RT. After three further washes in TBS/T for 5 minutes at RT proteins were revealed by luminol reaction with the ECL+plus westernblot detection system (Life Technologies) for 5 minutes at RT. Membranes were drained of excess of developing solution, wrapped in plastic foil and exposed to x-ray film. Detailed descriptions were provided previously (Narayanan et al., 2015).

Luciferase assay

Putative Pax6 binding sites in the promoter regions of the candidate genes (Ssx2ip, Wnt5a, Fgfr1, Celsr1, Pdgfrb, Cdc42ep1, Cdc42ep4) were identified from published data (Sansom et al., 2009), the respective regions were amplified from mouse genomic DNA and inserted into the pGL3 vector (Promega). These firefly luciferase-based reporter gene constructs were transfected along with a renilla expression vector into Neuro2A cells in a 24-well plate using Lipofectamine 2000 (Life Technologies). The cells were cultured for 48 h after which cell extracts were prepared and assayed for luciferase activity with the use of a Dual-Luciferase Reporter Assay System (Promega) following manufacturer's protocol, such that the firefly luciferase-based reporter gene activity was normalized to the renilla control in all cases.

In utero electroporation

In utero electroporation was performed as described previously (Tuoc et al., 2008, Tuoc et al., 2013) and detailed description is provided here. Soon before surgery, mix the plasmids with 0.05% FastGreen in PBS at a final ratio of ca. 4:1 and centrifuge the mixture for 2 min at 16,000 x g to remove all precipitates. Load the DNA mixture into a previously pulled borosilicate glass capillary. Pulling parameters using a P-97 pipette puller are: pull: 200; vel: 140; time: 140. Heat is given by a ramp test and depends on the specific lot of capillaries being used. Mount the capillary on the nozzle of the PDES pressure ejection system (NPI). Sterilize all surgery tools in a dry glass bead sterilizer (F.S.T.) and deeply anesthetize a pregnant mouse at stage E13.5 of gestation using an isoflurane

vaporizer (Harvard Apparatus). Place the animal in supine position on a heating platform (Harvard Apparatus) set at 37°C and keep under constant isoflurane administration through a nose cone. Disinfect skin of the abdomen by wiping with 70% ethanol, and inject carprofen (diluted in 0.9% NaCl) subcutaneously at 0.1 mg/kg concentration as pre-emptive analgesic. Using a set of fine forceps and scissors, a 2 cm longitudinal midline incision is then made along the linea alba to cut the skin and subsequently the underlying abdominal muscular wall to access the peritoneal cavity. Dispense in the peritoneal cavity ca. 2 ml of IUE solution (D-PBS containing 100 U/ml of pen/strep) pre-warmed at 37 °C and keep the solution on a heating block. Cover the mouse with sterile drap containing a fissure from which the uteri will be removed. Retract the incision using a tungsten retractor, identify the uterus and pull it out holding it with forceps between adjacent embryos and finally lay it down on the sterile drap. During the whole operation, rinse the uterus with IUE solution to moisturize the organ and body cavity and prevent dehydration of the animal. Handle the uterus carefully holding it between thumb and index and turn one embryo until its head is visible and oriented towards the operator. Identify the telencephalic hemispheres and inject one of them from the dorso-lateral side. Release 1-2 µl of the DNA solution (approximately 2 µg/µl, dissolved in water) using the footswitch of a PDES pressure ejection system (NPI) until the ventricle is outlined by FastGreen. Place the anode of the tweezer-type circular electrodes (3mm diameter) on the injection site and the cathode on the contralateral side and deliver 2-4 pulses of 30 V for 50 ms with 950 ms interval between each pulse using an electroporator (NEPA GENE) generating square-shaped electric fields operated through a footswitch. Avoid placing the electrodes close to the placenta as this may cause hemorrhage and damage the embryo. When all embryos are injected and electroporated, place the uterus back into the abdominal cavity and close the muscular walls with a suture string suturing every 3-4 mm. The knots should be snug to the muscle but not too tight to allow a little swelling of the tissue. Finally, close the overlying skin using metal clips. Disinfect the skin with 70% ethanol, remove the mouse from the isoflurane mask and transfer it in a housing cage when fully awake. Monitor the recovery of the mouse until locomotor behaviour is normal. The embryonic brains were harvested at E15.5 and checked for GFP signal using a fluorescent stereomicroscope. After this, the brains were processed for immunohistochemical analysis.

In IUE experiments shown in Figure, CMV-GFP plasmid was used as non-targeting control and CMV-GFP plasmid was co-injected with shCEP4 for knockdown at a ratio of 1:1 (2 µg/µl concentration). In rescue experiments shown in Figure, pCIG2-CEP4-ires-GFP plasmid was co-injected with shCEP4 at a

ratio of 1:1 (2 µg/µl concentration). In gain of function experiment shown in Figure, pCIG2-Foxn4-ires-GFP was injected at a concentration of 2 µg/µl concentration.

RNA-Sequencing

RNA was extracted (RNAeasy kit, Qiagen) from pallium from 4 control, 4 Pax6cKO_Emx1-Cre, 4 BAF155cKO_Emx1-Cre E15.5 littermate embryos. cDNA libraries were prepared with the TruSeq RNA Sample Preparation v2 Kit. The amount was measured in Nanodrop and the quality in Agilent 2100 Bioanalyzer. Base calling, fastq conversion, quality control, read alignment were all preformed as outlined for ChIP-Seq. Reads were aligned to mouse genome mm10 and counted with FeaturesCount (http://bioinf.wehi.edu.au/featureCounts/). Differential expression was assessed using DESeq2 from Bioconductor (Love et al., 2014). Functional GO enrichment analysis was performed with ToppGene (Chen et al., 2009).

Analysis of the orientation of cell division

Cortical sections were stained with pVim, a cytoplasmic marker to identify RG cell shape and process and pHH3, a nuclear marker to identify dividing cells at anaphase and early telophase. Images of z-stack sections were taken by SP5 confocal microscopy and the plane of division respective to the ventricular surface was analysed: angles from 90-60° were interpreted as vertical, 60-30° as oblique and 30-0° as horizontal divisions. (Postiglione et al., 2011; Tuoc et al., 2013).

Magnetic Resonance Imaging

MRI was performed *ex vivo* on the brain of five wildtype and four BAF155cKO mice at the age of 8 weeks at 9.4 T (Bruker Biospin MRI GmbH, Ettlingen, Germany). Radiofrequency excitation and signal reception were accomplished with the use of a birdcage resonator (inner diameter 72 mm) and a 4-channel phased-array surface coil, respectively (both Bruker Biospin MRI GmbH, Ettlingen, Germany). Three-dimensional proton-density-weighted MRI was performed with a 3D gradient-echo sequence (radiofrequency-spoiled FLASH, repetition time = 22 ms, echo time = 7.6 ms, flip angle = 15°, fat suppression = 90°, measuring time = 66 min.) at an isotropic resolution of 100 µm. For evaluation of signal intensities, anatomically defined cross-sections were obtained from the original 3D MRI data sets by multiplanar reconstructions using software supplied by the manufacturer (Paravision 5.0, Bruker Biospin MRI GmbH, Ettlingen, Germany). The plane crossing the anterior as well as posterior commissure served as a reference for the selection of standardized sections to facilitate comparisons

with minimized intra- and interindividual variability. The analysis followed a strategy previously developed for intra- and inter-individual comparisons of MR images.

Image acquisition and quantification

Images were captured with an Axio Imager M2 (Zeiss) with a Neurolucida system (Version 11; MBF Bioscience) and confocal fluorescence microscope (TCS SP5; Leica). All images were processed with Adobe Photoshop (Version CS6) by overlaying the pictures, adjusting brightness, contrast and size. For all cell countings, the sections among the experimental groups (n = 3 per group) were chosen such that they are comparable in the rostro-caudal and laterio-medial axes. For cell counts in sections from WT and BAF155cKO cortices for various markers, the positive cells in the specified zone were counted within equally sized frames of the respective cortical regions (entire neocortex or lateral cortex). For cell counts in sections from IUE experiments, single plane confocal images were used to verify co-localization of multiple fluorescent signals. The number of double positive cells within equally sized frames were counted by Neurolucida system.

Statistical analysis

For all data sets, the arithmetic average and the standard deviation were calculated. Error bars depict the standard deviation. The Student's t-test or one-way ANOVA followed by Tukey-Kramer's post hoc analysis was used to examine whether data sets differed significantly. Data were considered as significant with $p<0.05$ and as highly significant with $p<0.001$. Calculations of the arithmetic average, the standard deviation and t-test were performed with Microsoft Excel. The significance of the obtained data was tested using the program Sigmaplot v12.0.

Results

Expression of BAF155 in mouse cortical progenitors and conditional inactivation of *BAF155 in vivo*

Previous studies from our group showed that the expression of BAF170 is dynamic during mouse cortical development and predominantly found in differentiated cells. However, cortical progenitors displayed strong BAF170 expression in early stages (E10.5-14.5) followed by a near absence during E15.5-16.5 and re-appearance in late stages (E17.5-18.5). Interestingly, loss of BAF170 expression in the cortex resulted in tremendous increase in BAF155 expression, indicating a competition between the two core subunits (Tuoc et al., 2013). In order to characterize the expression pattern of BAF155 during cortical development, we performed immunohistochemistry (IHC) on wildtype mouse cortical sections from E13.5, E15.5 and E18.5 embryos with BAF155 antibody. At E15.5, BAF155 is exclusively expressed in the ventricular zone of both dorsal (cortex) and ventral (basal ganglia) telencephalon (Fig. 1A). In addition, we also observed that BAF155 is either absent or expressed at very low levels during earlier (E13.5) and later (E18.5) stages of cortical development (Fig. 1B). In order to define the population of progenitors that express BAF155 in the mouse neocortex, we performed triple-IHC on cortical sections from E15.5 wildtype embryos with antibodies for BAF155 and markers for subtype of cortical progenitor, including RGs (Gotz et al., 1998) and IPs (Hevner et al., 2006). BAF155 co-localized strongly with RG marker Pax6 in VZ (Fig. 1C) in comparison to the IP marker Tbr2 (Fig. 1D). Interestingly, among the IP population, sub-apical IPs expressed relatively higher levels of BAF155 (Fig. 1D, arrow) whereas the expression was either low or completely absent in IPs in basal regions of SVZ (Fig. 1D, arrowhead). Taken together, these findings indicate that BAF155 displays a dynamic temporal expression pattern during cortical development, interestingly complementary to that of BAF170. Although BAF155 is expressed in both cortical progenitor populations, it is strongly expressed in vRGs and sub-apical IPs.

To address the functions of BAF155 *in vivo*, we generated *BAF155* knockout mice by crossing floxed *BAF155* (*BAF155*$^{fl/fl}$) mice (Choi et al., 2012), with an *Emx1-Cre* line, in which Cre-recombinase is driven in cortical progenitors starting at E9.5, reaching full recombination activity before E12.5 (Gorski et al., 2002). The efficiency of Cre-mediated recombination was verified in E15.5 brain sections by IHC using an anti-BAF155 antibody. The results revealed a complete loss of BAF155 protein in the pallium of *BAF155*$^{fl/fl}$*;Emx1-Cre* embryos, confirming *BAF155* knockout (Fig. 2A). The term "*BAF155*cKO" was

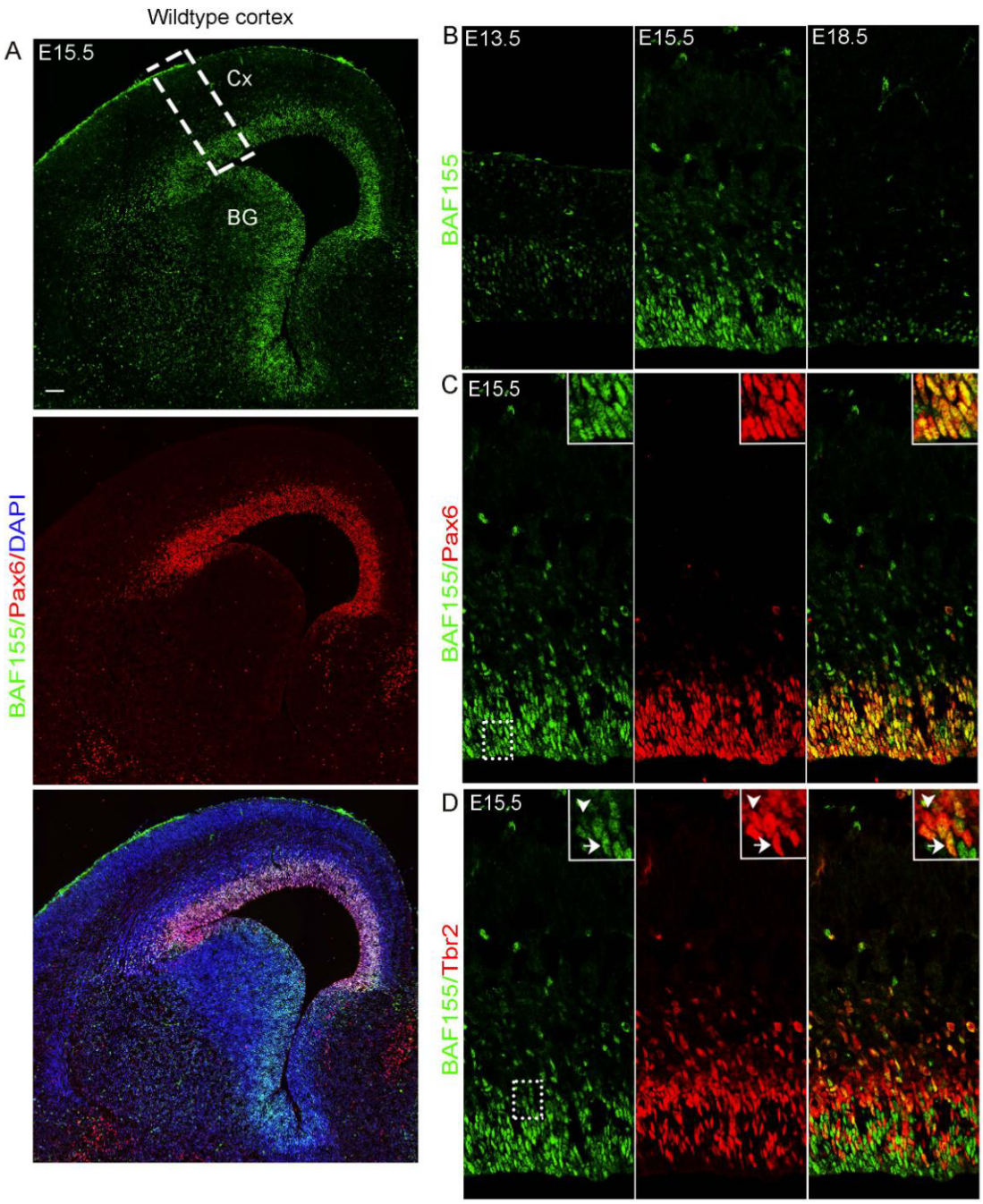

Figure 1. Expression of BAF155 in developing cerebral cortex

(A) Double IHC using antibodies against BAF155 (green) and Pax6 (red) shows a high expression of BAF155 in the proliferative zones of both dorsal (cortex, Cx) and ventral (basal ganglia, BG) telencephalon. (B) IHC using anti-BAF155 antibody during different stages of cortical development. High magnification images from lateral cortex (corresponding to the white frame from A) shows very low levels of BAF155 during E13.5 & E18.5, whereas high levels at E15.5. (C) Double IHC using antibodies against BAF155 (green) and RG marker Pax6 (red) followed by confocal imaging of lateral cortex showed strong co-localization of the markers at E15.5. Higher magnification of the VZ (white box) is presented in the inner panel. (D) Double IHC using antibodies against BAF155 (green) and IP marker Tbr2 (red) followed by confocal imaging of lateral cortex showed weak co-localization of the markers at E15.5. Higher magnification of the SVZ (white box) is presented in the inner panel. Sub-apical IP expresses relatively high levels of BAF155 (white arrow), whereas basal IP expresses lower levels (white arrow head). [Abbreviations: VZ, ventricular zone; SVZ, subventricular zone; RG, radial glia; IP, intermediate progenitor]. Scale bar = 100μm.

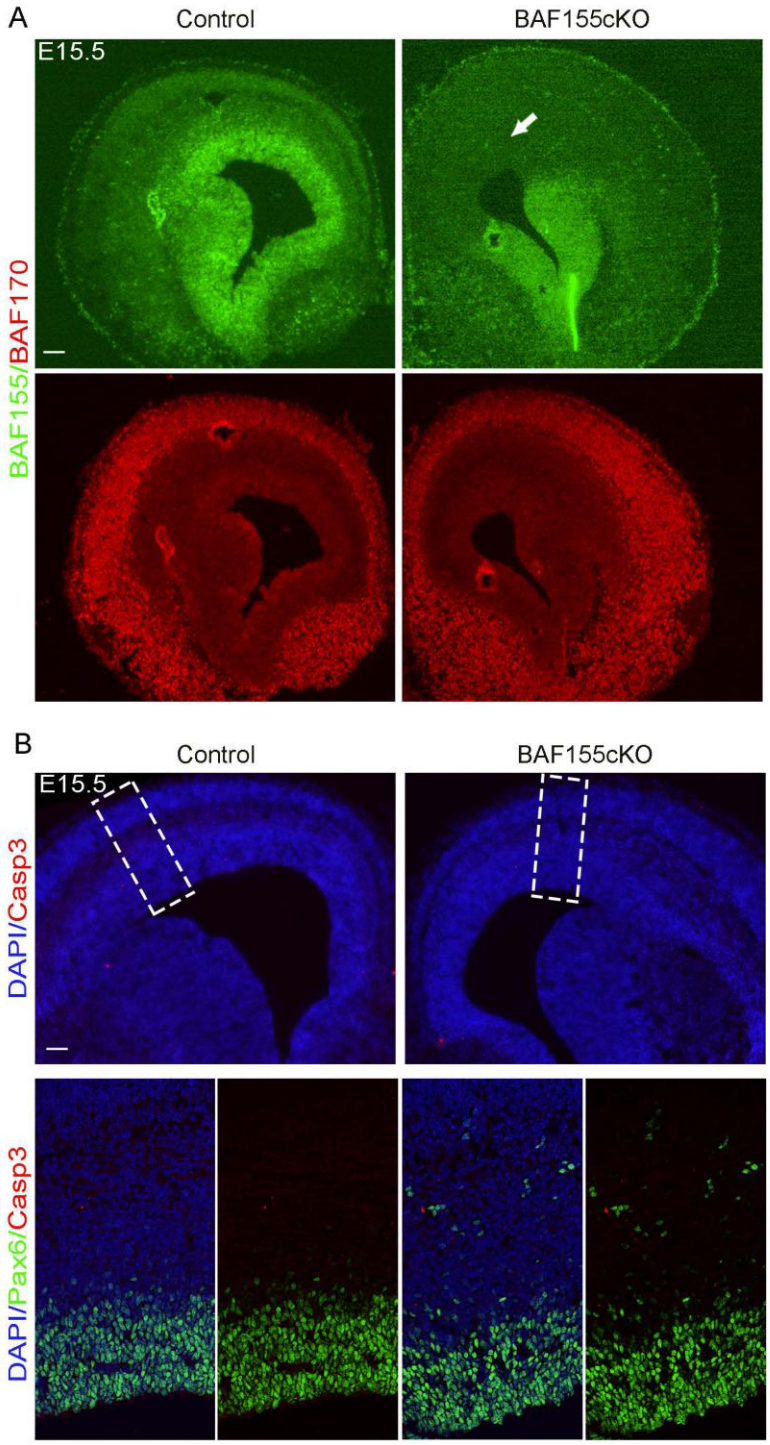

Figure 2. Expression of BAF155 and BAF170 in mutant cortices

(A) IHC using antibodies against BAF155, BAF170 at E15.5 showed complete loss of BAF155 expression in pallium (cortex; white arrow) of BAF155cKO compared to control, whereas the expression in sub-pallium remains unaltered (upper panel). However, the expression of BAF170 is unaltered in the BAF155cKO cortex compared to control.

(B) IHC using antibodies against cleaved Caspase3 and Pax6 at E15.5 showed no obvious increase in apoptosis both in the entire cortex and specifically in the RG population. Overview images are shown in the upper panel and high magnification confocal image of the lateral cortex (white frame) is shown in the lower panel. [Abbreviations: Cx, cortex; BG, basal ganglia]. Scale bars = 100µm.

used for all subsequent references to *BAF155*$^{fl/fl}$*;Emx1-Cre* embryos. The resulting *BAF155*cKO mice were viable, healthy, fertile, and reached adulthood. We noted that while activation and inactivation of BAF170 profoundly affects the expression of BAF155 in cortical tissues, the expression of BAF170 is however largely preserved in BAF155cKO cortex (Fig. 2A). Finally, through cleaved-Caspase3 IHC, BAF155cKO mice showed no increase in apoptosis both in the entire cortex and specifically in the RG cell population (Fig. 2B).

BAF155 control expression of a large set of Pax6-dependent genes, possibly by potentiating Pax6 transcriptional activity.

In a previous study, we found that Pax6 interacts with multiple BAF subunits, including Brm, BAF170 and BAF155 in cortical progenitors (Tuoc et al., 2013). We set out to find if the interaction between BAF155 and Pax6 influences Pax6-dependent transcriptional activity using a Pax6-dependent reporter vector (pCON/P3) (Epstein et al., 1994; Tuoc and Stoykova, 2008). We generated primary cortical neural stem cell (NSC) culture from BAF155cKO and control embryos. We nucleofected pCON/P3 plus eGFP plasmids into the NSCs and examined the expression level of luciferase by western blot (WB) analysis after 2 days *in vitro* (DIV). We found that the loss of BAF155 in NSCs from BAF155cKO embryos led to a profoundly reduced expression level of luciferase as compared to those from control (Fig. 3A/B). To determine if BAF155 controls the level of Pax6-dependent transcriptional activity *in vivo*, we electroporated pCON/P3 plus eGFP plasmids into E13.5 brains of BAF155cKO and control mice, and after one day cortical tissues were examined by WB for Luciferase expression. Protein quantification by WB revealed that BAF155cKO cortices contained 23% less amount of Luciferase protein than that in control (Fig. 3A/B). Thus, our data indicated that BAF155 is required for normal Pax6-dependent transcriptional activity.

In our attempt to gain further insights into the functional interaction between BAF155 and Pax6 during cortical development, transcriptomic analysis of E15.5 cortices of *BAF155*cKO_Emx1-Cre and *Pax6*cKO_Emx1-Cre embryos was performed (in collaboration with the groups of Prof. Andre Fischer & Dr. Stefan Bonn, DZNE, Goettingen) to determine gene expression changes (Fig. 3C/D). In BAF155cKO cortex, there were 1179 down- and 939 up-regulated genes, whereas in Pax6cKO cortex those numbers were 2965 and 2415 respectively (p-value < 0.01 & |fold change| > 1.2) (Fig. 3C/D). Furthermore, we noticed considerable overlap between a number of BAF155 and Pax6-regulated genes with altered expression in BAF155cKO and Pax6cKO E15.5 cortices (Fig. 3E/F). Gene ontology (GO) analysis of the RNA-seq data indicated substantial enrichment of genes important in a wide-

range of developmental processes. Notably, both BAF155 and Pax6 control expression of genes related to forebrain development, neurogenesis, and neuron differentiation among others (Fig. 3G). Taken together, our finding suggested that BAF155 control expression of a large set of Pax6-dependent genes, possibly by potentiating Pax6 transcriptional activity.

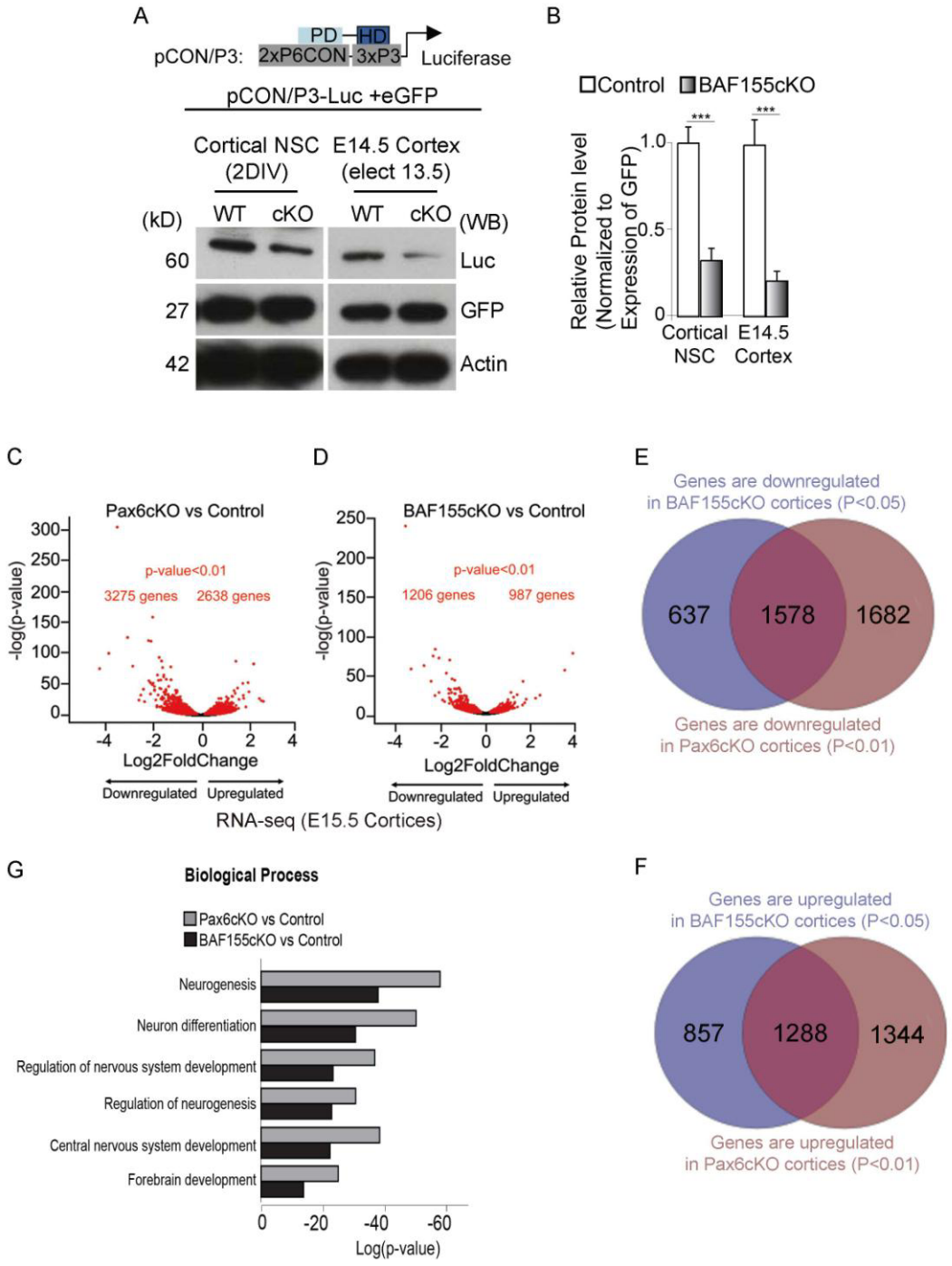

Figure 3. BAF155 and Pax6 co-regulate global gene expression program in developing cerebral cortex

Figure 3. BAF155 and Pax6 co-regulate global gene expression program in developing cerebral cortex
(A-B) Reporter assay was performed using pCON/P3 construct containing Pax6 binding motifs that drives Luciferase expression. The construct was both transfected to cortical NSC and electroporated into E13.5 embryos and samples were collected 2 DIV and 1 DPE respectively for western blotting (A). In both cases, there is a significant reduction in luciferase activity in BAF155cKO compared to control (B).
(C-D) RNA sequencing was performed in E15.5 BAF155cKO and Pax6cKO cortices. Graphs depict the number of both down- and up-regulated genes in BAF155cKO (C) and Pax6cKO (D).
(E-F) The overlap between genes down- (E) and up-regulated (F) in BAF155cKO and Pax6cKO embryos.
(G) Gene ontology analysis revealed that both BAF155 and Pax6 regulates key genes involved in forebrain development, neurogenesis and neuron differentiation. [Abbreviations: NSC, neural stem cell; DIV, days in vitro; DPE, days post electroporationventricular zone].

BAF155 control genesis of intermediate progenitors (IPs)

Earlier studies have identified Pax6 as a RG-specific transcription factor that determines choice of the indirect mode of cortical neurogenesis and genesis of IPs (Georgala et al., 2011; Gotz et al., 1998; Quinn et al., 2006; Sansom et al., 2009; Thakurela et al., 2016; Tuoc et al., 2013; Tuoc et al., 2009). As expected, expression of many IP genes in our RNA-seq experiment is downregulated in Pax6cKO cortex (Fig. 4A). Remarkably, expression of all known IP genes was also reduced in BAF155cKO cortex in RNA-seq analysis (Fig. 4B). We then looked into the production of IPs in BAF155cKO cortex by examining the expression of IP marker Tbr2 (Hevner et al., 2006), and Ngn2, a marker for cells in transition between RGs and IPs, whose expression is necessary for IP identity (Arnold et al., 2008; Ochiai et al., 2009; Pinto et al., 2009; Sessa et al., 2008). We found that in BAF155cKO embryos, the number of Tbr2+ IPs and Ngn2+ cells was substantially diminished as compared to control in caudo-lateral cortex (Fig. 4C-F). Thus, these findings indicated that together with transcription factor Pax6, chromatin remodeling BAF155 subunit acts as an upstream regulator of IP genesis in the cerebral cortex.

Ectopic distribution of cortical progenitors in BAF155 deficient cortex

Although the total number of Tbr2+/Ngn2+ IPs is lower in BAF155cKO as compared to control; notably, an ectopic presence of Tbr2+/Ngn2+ cells was seen in intermediate zone (IZ) and cortical plate (CP) of the mutants (Fig. 4C/D, white arrow). Intrigued by this finding, we characterized the number and location of RG cell population in BAF155cKO mutants, by using both nuclear (Pax6, Sox2) and cytoplasmic (GLAST, BLBP) RG markers (Feng et al., 1994; Shibata et al., 1997). Interestingly, similar to the IP cell population, there is a significant ectopic RG cell population that are Pax6+ (Fig. 5A/B), Sox2+/GLAST+ (Fig. 5C/E) and AP2ɤ+/BLBP+ (Fig. 5D/E) in the IZ/CP of BAF155cKO cortex. We also observed that these ectopic RGs were expressing pVim (cytoplasmic marker for dividing RGs) and pHH3 (nuclear marker for dividing cells) with a clear pia-directed basal process (Fig. 5F, white arrow-heads).

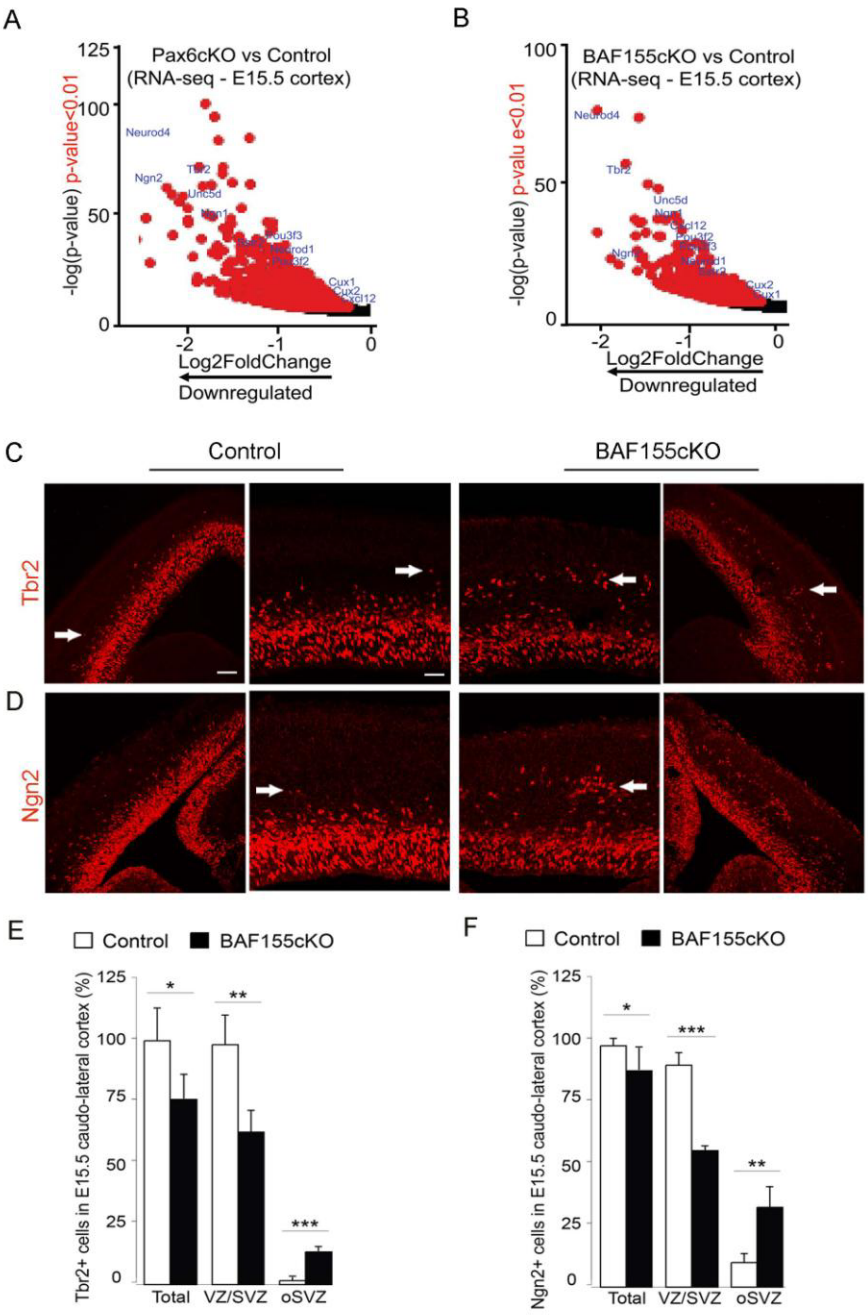

Figure 4. BAF155 deficient cortex results in decrease of intermediate progenitors at SVZ

(A, B) Among genes that had downregulated expression in RNA-seq analyses of E15.5 Pax6cKO (A) and BAF155cKO (B) cortices, we found several genes with known functions in IP genesis. (C) IHC using antibody against IP marker Tbr2 on coronal sections of E15.5 control (left) and BAF155cKO (right) cortices. Higher magnification is presented in the middle panels. Note the presence of Tbr2+ IPs in ectopic basal locations (White arrows). (D) IHC using antibody against Ngn2 (a marker for cells in transition between RG and IP fate) on coronal sections of E15.5 control (left) and BAF155cKO (right) cortices. Higher magnification is presented in the middle panels. Note the presence of Ngn2+ cells in ectopic basal locations (White arrows). (E-F) Statistical analysis of the number of Tbr2+ (E) and Ngn2+ (F) cells, comparing BAF155cKO and control caudo-lateral cortices at E15.5. It should be noted that as compared to control, a diminished number of Tbr2+ and Ngn2+ cells are found both in total and in SVZ. However, an increased number of Tbr2+ and Ngn2+ cells in oSVZ was found in BAF155cKO cortex. Values are presented as means ± SEMs (*0.01<P<0.05, **0.001<P<0.01, ***P <0.001). [Abbreviations: VZ, ventricular zone; SVZ, subventricular zone; oSVZ, outer subventricular zone; IZ, intermediate zone; CP, cortical plate; IP, intermediate progenitor]. Scale bar = 100µm.

To further characterize the occurrence and abundance of RGs in detail, we quantified the number of Pax6+ cells in BAF155cKO cortex at E15.5 in rostral, medial and caudal cortices. The boundaries between the VZ/SVZ and IZ/CP from E15.5-E18.5 can be easily distinguished through the expression of Tau-1 or Tuj1 (Martinez-Cerdeno et al., 2012) (Fig. 6A). This basal region of the mouse cortex, positive for Tau-1 or Tuj1 immunoreactivity, is referred to as "outer SVZ (oSVZ)" in our analyses, due to its peculiar similarity to the distinctly basal progenitor abundant oSVZ found in primate cortex.

Our analysis revealed that total number of Pax6+ RGs was not significantly different between the control and BAF155cKO cortices. However, the number of Pax6+ ventricular RGs (vRGs) was significantly diminished together with a remarkable increase in basal RGs (bRGs) in the oSVZ (Fig. 5A/B). Additionally, we observed that these Pax6+ bRGs are distributed in a gradient, such that rostro-lateral, medio-dorsal and caudo-medial regions of the cortex have the highest numbers (Fig. 6B). Thus, in BAF155cKO embryos, oSVZ cortical progenitors are distributed more frequently in somatosensory areas than other cortical areas, which is consistent with previous report in WT embryos (Wang et al., 2011).

In order to ascertain that these findings are progenitor-specific, we created a cortical neuron-specific knockout of BAF155 by using Nex-Cre (Goebbels et al., 2006). The selective deletion of BAF155 in post-mitotic neurons did not influence the location of cortical progenitors (Fig. 7A), indicating that post-mitotic expression of BAF155 plays no critical role in genesis of cortical progenitor subtypes. In addition, deletion of BAF155 in late cortical progenitors using hGFAP-Cre which is active from E13.5 (Zhuo et al., 2001), also resulted in no ectopic presence of progenitors in the oSVZ (Fig. 7B). Taken together, these results indicated that the loss of BAF155 exclusively in early cortical progenitors induces genesis of primate-like bRGs having a distinct pia-directed basal process.

Ablation of BAF155 has mild effect on cortical layer formation

Given the significant loss of IPs and ectopic distribution of cortical progenitors in the oSVZ, we wanted to determine if this has any consequence on neuronal migration and cortical lamination. To this end, we first performed IHC on E18.5 cortices of control and BAF155cKO with markers for early-born lower layer (LL) neurons (Ctip2) and late-born upper layer (UL) neurons (Satb2). The IHC analysis showed that both the UL and LL are well formed in the BAF155cKO cortex and there is no evident abnormality in neuronal migration (Fig. 8A).

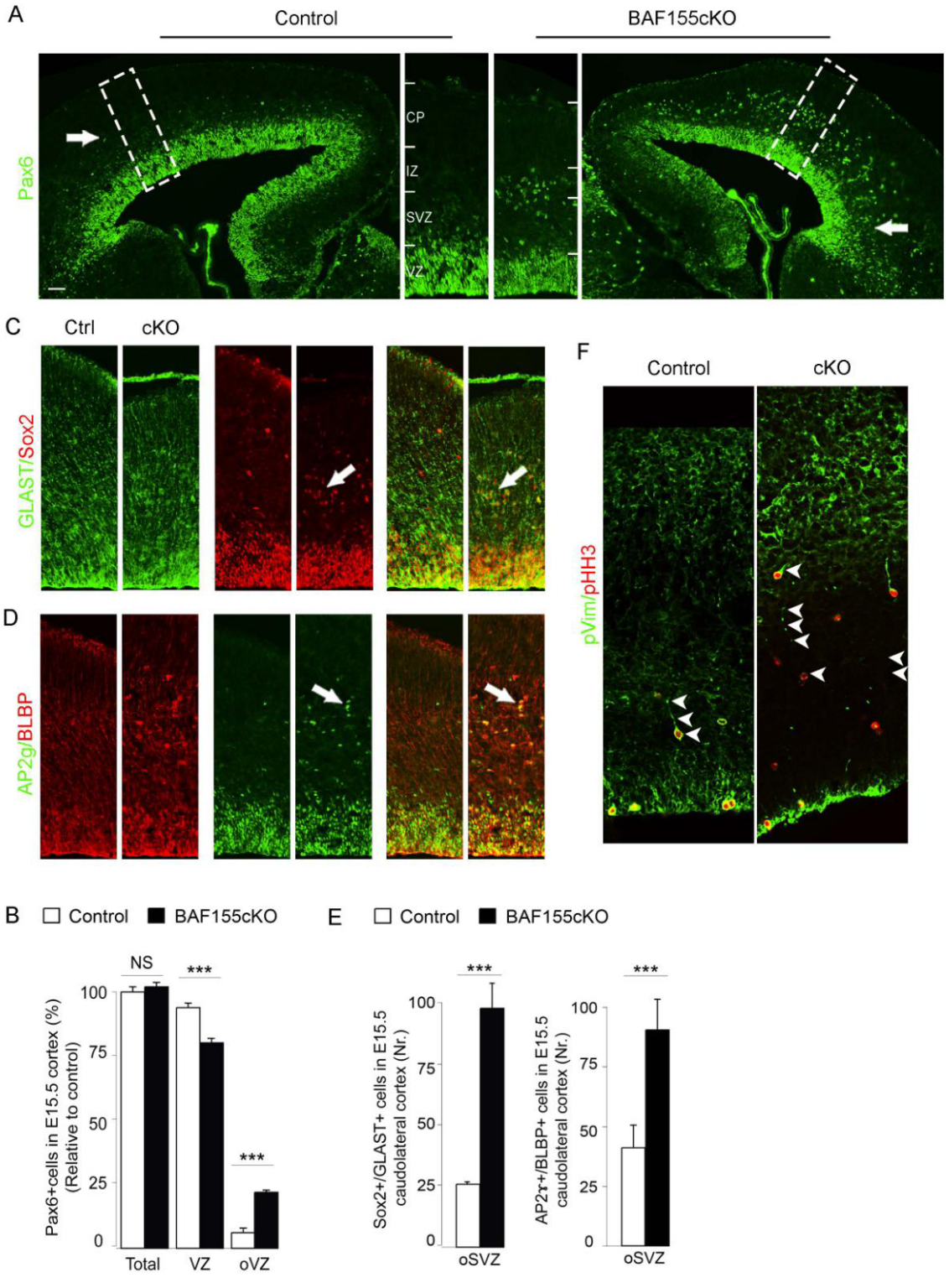

Figure 5. BAF155 deficient cortex displays increased basal radial glial progenitors

Figure 5. BAF155 deficient cortex displays increased basal radial glial progenitors
(A) IHC using antibody against RG marker Pax6 on coronal sections of E15.5 control (left) and BAF155cKO (right) cortices. Note the presence of Pax6+ RGs in ectopic basal locations (White arrows). Higher magnification of the corresponding lateral cortices highlighted by white frame is presented in the middle panels. Note the presence of Pax6+ RGs in IZ of the mutant cortex. (B) Statistical analysis of the total number of Pax6+ RGs comparing BAF155cKO and control cortices across rostral, medial and caudal regions at E15.5. Though the total number of Pax6+ RGs remains unaffected, it should be noted that compared to control, a diminished number of Pax6+ RGs in VZ and an increased number of Pax6+ RGs in oSVZ was found in BAF155cKO cortex. (C) IHC using antibody against nuclear (Sox2) and cytoplasmic (GLAST) RG marker on coronal sections of E15.5 control (left) and BAF155cKO (right) cortices. Higher magnification of the corresponding lateral cortices is presented. Note the ectopic presence of Sox2+/GLAST+ RGs in basal locations of BAF155cKO cortex (White arrows). (D) IHC using antibody against nuclear marker for cells in transition between RG and IP fate (AP2g) and cytoplasmic RG marker (BLBP) on coronal sections of E15.5 control (left) and BAF155cKO (right) cortices. Higher magnification of the corresponding lateral cortices is presented. Note the ectopic presence of AP2g+/BLBP+ RGs in basal locations of BAF155cKO cortex (White arrows). (E) Statistical analysis of the total number of Sox2+/GLAST+ (left panel) and AP2g+/BLBP+ cells (right panel) showed significant increase in the oSVZ of BAF155cKO compared to control caudo-lateral cortices at E15.5. Values are presented as means ± SEMs (***P <0.001). (F) IHC using antibody against pVim (marker for dividing cells) and pHH3 (marker for dividing nucleus) on coronal sections of E15.5 control (left) and BAF155cKO (right) cortices. Higher magnification of the corresponding lateral cortices is presented. Note the pia-directed basal process stained for pVim in basal locations of BAF155cKO cortex (White arrowheads). Scale bar = 100µm.

To precisely assess the consequence of BAF155 mutagenesis on cortical size and thickness, we employed *ex vivo* structural magnetic resonance imaging (MRI) (in collaboration with the group of Dr. Jens Frahm, BiomedNMR, Goettingen). The entire thickness, size and surface area of the cerebrum were not significantly different between adult (P56) BAF155cKO and control mice (Fig. 8B-D).

The regional differences in the abundance of bRGs in BAF155cKO mutants (Fig. 6B) prompted us to quantify the number of cortical neurons generated in the BAF155cKO cortex at P7 in different cortical areas, including rostral, somatosensory and caudal areas of lateral and medial cortices. We found that the loss of BAF155 largely did not affect the number of Tbr1+ (Fig. 9A-C) and Ctip2+ (Fig. A/B) LL neurons in all examined cortical areas. Remarkably, the number of Tbr1+ (Fig. 9A-C) and Brn2+ (Fig. 10C/D) UL neurons in rostral area of lateral cortex and somatosensory area of medial cortex was increased in mutant compared to that of control. Collectively, these findings suggested that the BAF155cKO cortex, with a diminished pool of IPs and increased number of bRGs, displays normal neurogenesis in most cortical areas. However, resulting from the gradient distribution of bRGs in the embryonic cortex, enhanced neuronal output is observed in somatosensory area of BAF155cKO mutants.

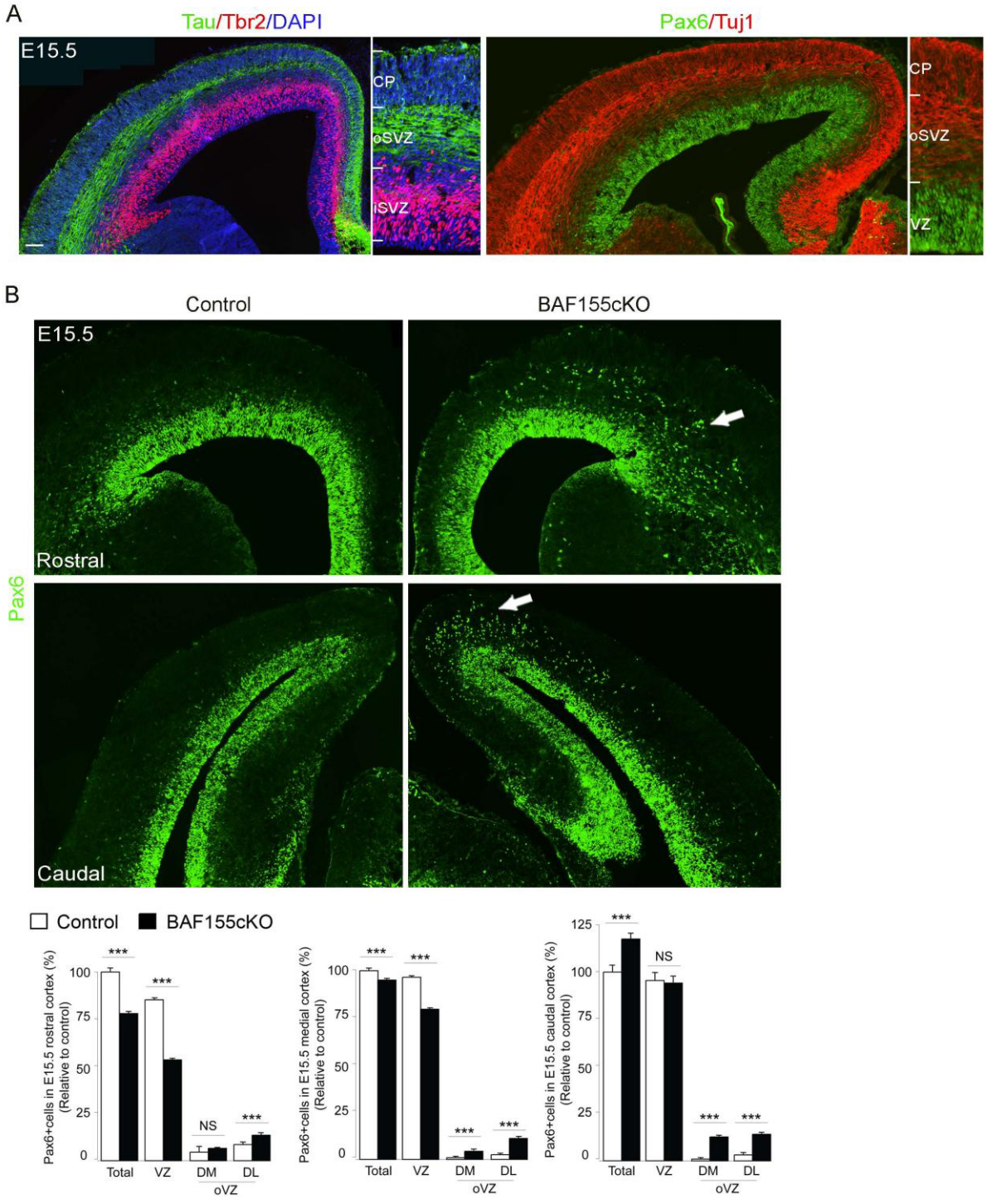

Figure 6. Basal radial glia are distributed in a gradient across rostro-caudal axis of BAF155cKO cortex

(A) IHC using antibodies against Tau/Tbr2 (left panel) and Tuj1/Pax6 (right panel) in E15.5 mouse cortex distinguishes VZ/SVZ from the rest of the cortex. The region displaying dense fibers running parallel to apical surface and positive for Tau/Tuj1 markers are identified as oSVZ.

(B) Pax6 IHC at E15.5 rostral, medial and caudal sections of BAF155cKO and control cortices showed a gradient distribution of RGs. Relatively higher numbers of RGs were found in rostro-lateral, medio-dorsal and caudo-medial regions (white arrows) of the BAF155cKO cortex. The corresponding graphs in the right panel show statistical analyses. Values are presented as means ± SEMs (***p <0.001). Scale bars = 100µm.

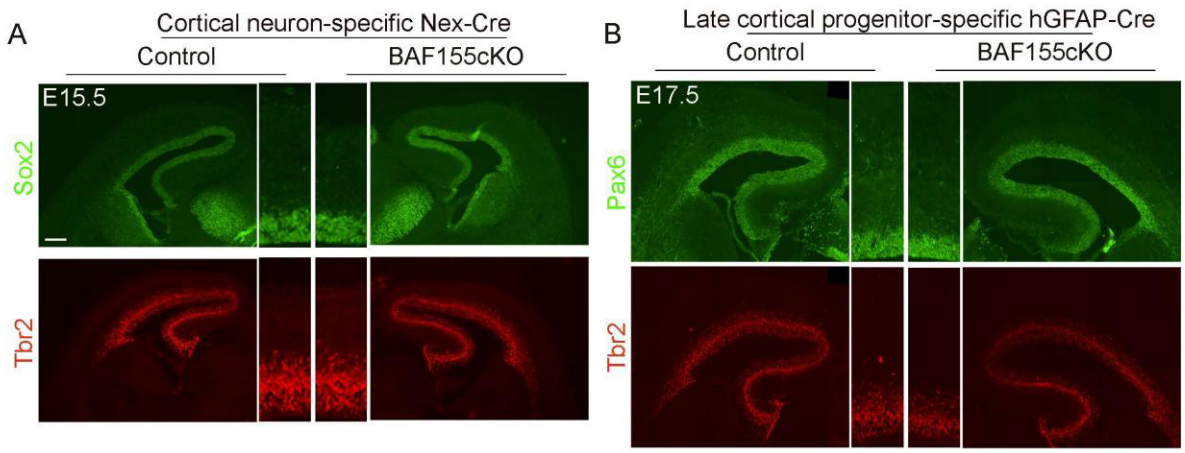

Figure 7. BAF155 regulates basal progenitor genesis through progenitor-specific role during early corticogenesis

(A) IHC using antibodies against Sox2 (RG marker) and Tbr2 (IP marker) in E15.5 control and BAF155cKO_NexCre cortices. Higher magnifications of the lateral cortex are presented in the middle panels. Deletion of BAF155 using cortical neuron-specific Cre generated no basal progenitor, thereby showing that BAF155 has a progenitor-specific role in basal progenitor genesis.

(B) IHC using antibodies against Pax6 (RG marker) and Tbr2 (IP marker) in E15.5 control and BAF155cKO_hGFAPCre cortices. Higher magnifications of the lateral cortex are presented in the middle panels. Deletion of BAF155 using late cortical progenitor-specific Cre generated no basal progenitor, thereby showing that BAF155 has a role in basal progenitor genesis only during early corticogenesis. Scale bars = 100µm.

Loss of BAF155 or Pax6 altered the mode of RG cell division and induces genesis of BPs preferably in non cell-autonomous manner.

Earlier studies have shown that deletion of Pax6 affected the morphology, proliferation and cell division of vRGs (Gotz et al., 1998). More recently, Pax6 has also been implicated in the ectopic distribution of cortical progenitors in the IZ/CP and genesis of primate-like bRGs (Asami et al., 2011; Wong et al., 2015). Since, the BAF155cKO cortex also consists of BPs, we were interested to determine if BAF155 and Pax6 act in the same genetic pathway in specifying BPs during cortical development. To this end, we sought to compare the number of bRGs in VZ and oSVZ in mouse cortex deficient for either Pax6 or BAF155 or both by generating cortex-specific single (cKO) and double (dcKO) mutants for these genes.

Because of the severe down-regulation of Sox2 and GLAST expression in Pax6cKO cortex, we then compared the number of Sox2+/GLAST+ RGs in VZ and oSVZ in BAF155cKO, dcKO and control cortices at E15.5 (Fig. 11A/B). The number of Sox2+/GLAST+ RGs in VZ of BAF155cKO tend to be lesser than that of control, although statistically non-significant, and the additional loss of Pax6 in dcKO lead to significant reduction of this cell population (Fig. 11B). On the other hand, both the BAF155cKO and

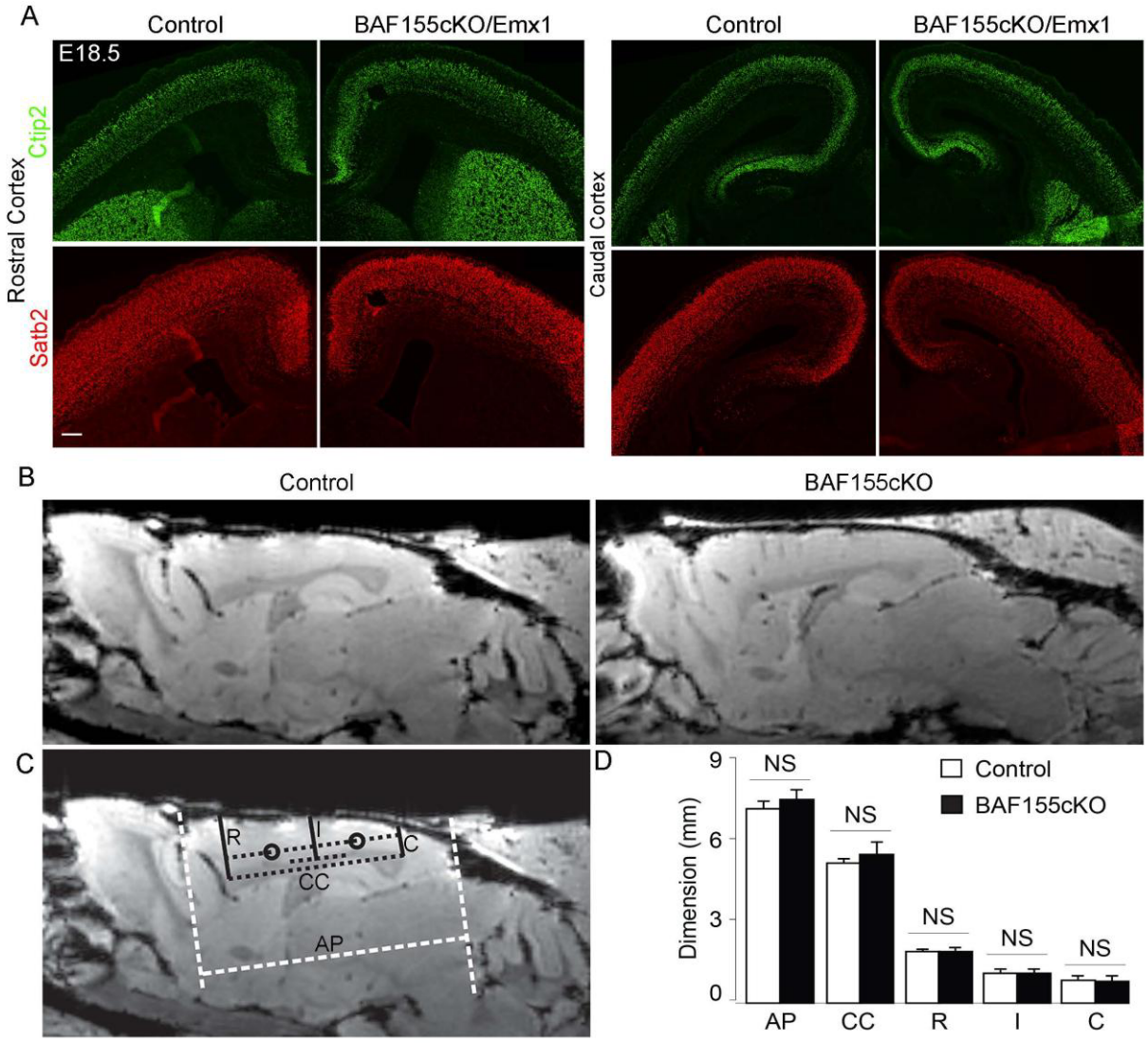

Figure 8. BAF155cKO cortex displays normal neuronal migration and cortical lamination

(A) IHC analysis using antibodies against LL (Ctip2) and UL (Stab2) neuronal markers in rostral (left) and caudal (right) sections of control and BAF155cKO cortices at E18.5 shows no significant abnormalities in neuronal migration and cortical lamination.

(B) Representative images of P28 control and BAF155cKO cortices obtained from magnetic resonance imaging (MRI).

(C-D) The longest white dashed line is the "AP length". The longest black dashed line is the "CC length". “R”, “I” and “C” denotes the distance between CC and pial surface at rostral, intermediate and caudal locations (cortical thickness) respectively (C). None of the above parameters were significantly different comparing control and BAF155cKO cortices (D). Scale bar=100µm.

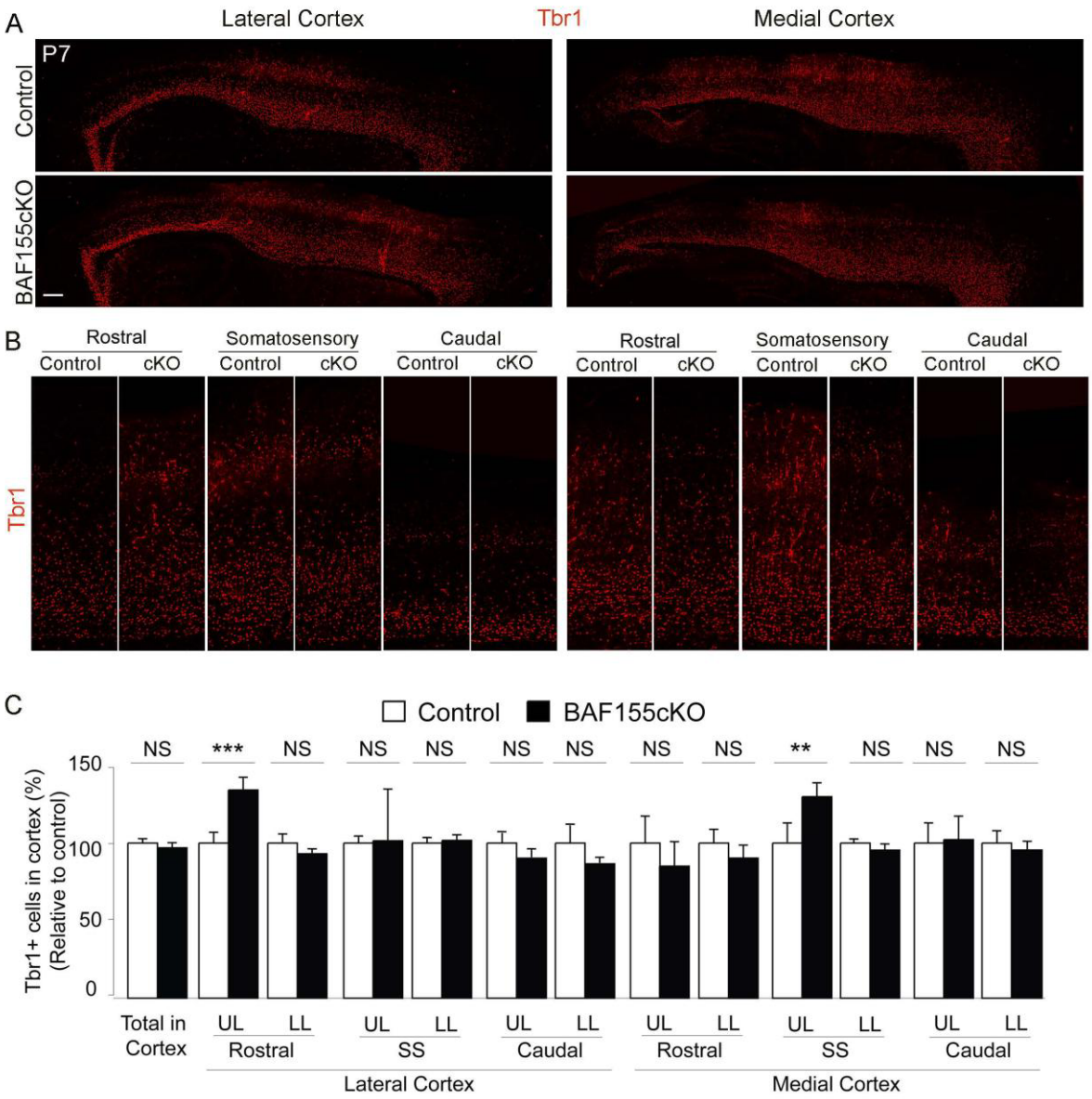

Figure 9. Deletion of BAF155 has only mild effect on both lower and upper layer neurons

(A) Overview images of P7 sagittal sections of control and BAF155cKO lateral (left panel) and medial (right panel) cortices immunostained for Tbr1, neuronal marker that labels distinct populations both in the upper and lower layers.

(B) Higher magnification images of rostral, somatosensory and caudal regions of the respective control and BAF155cKO cortices shown in A.

(C) Quantification of Tbr1+ cells in control and BAF155cKO cortices at P7 showed no significant difference in total number from lateral and medial regions. However, the Tbr1+ UL neurons are higher in rostro-lateral and medio-medial regions of the mutant cortex. Values are presented as means ± SEMs (**0.001<P<0.01, ***P <0.001). Scale bar=100µm.

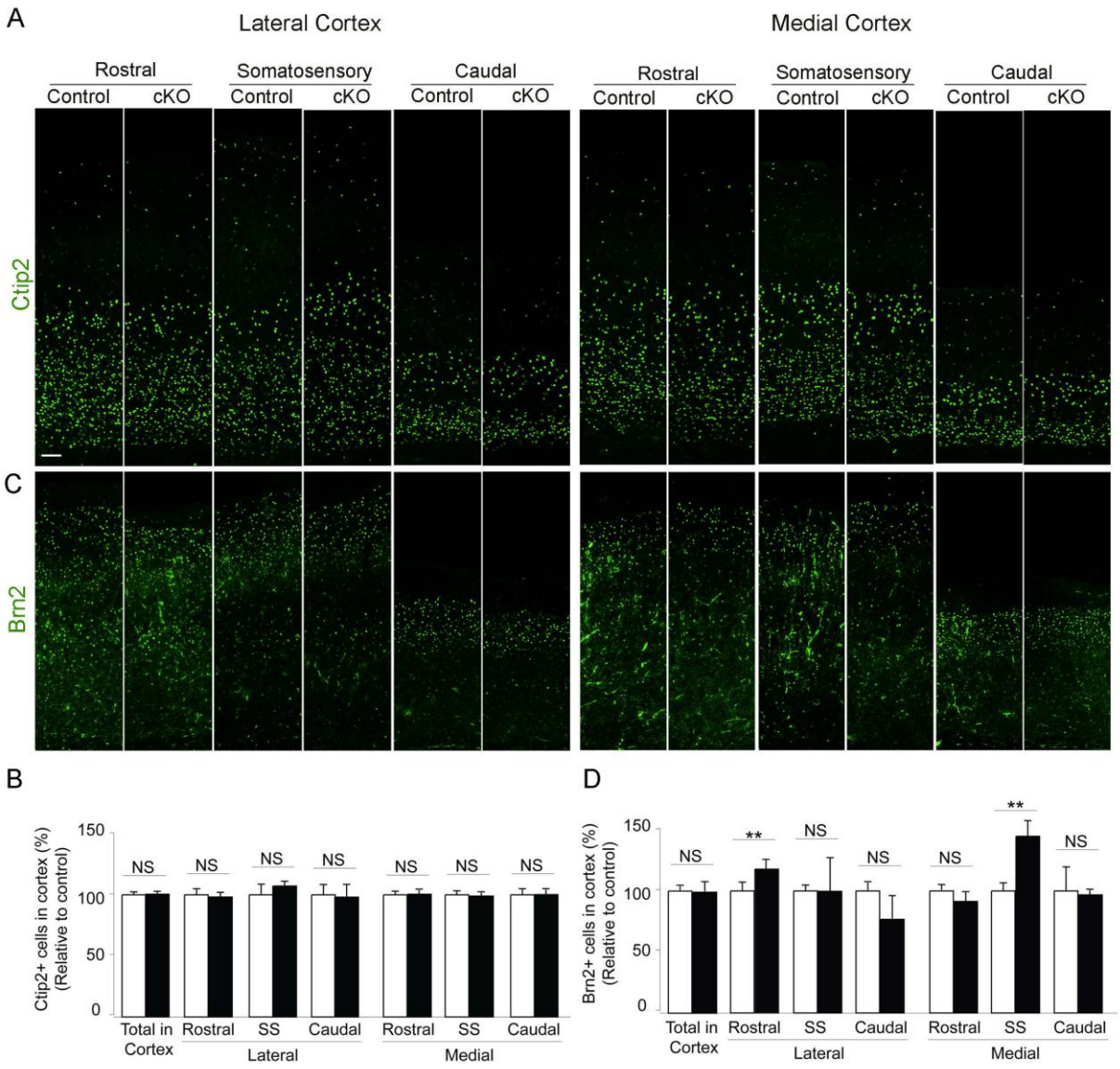

Figure 10. BAF155cKO cortex displays region-specific increase in upper layer neurons

(A) Higher magnification images of rostral, somatosensory and caudal regions of the respective control and BAF155cKO cortices immunostained for Ctip2, neuronal marker that labels lower layers.

(B) Quantification of Ctip2+ cells in control and BAF155cKO cortices at P7 showed no significant difference in total number from lateral and medial regions.

(C) Higher magnification images of rostral, somatosensory and caudal regions of the respective control and BAF155cKO cortices immunostained for Brn2, neuronal marker that labels upper layers.

(D) Quantification of Brn2+ cells in control and BAF155cKO cortices at P7 showed no significant difference in total number from lateral and medial regions. However, the Brn2+ UL neurons are higher in rostro-lateral and medio-medial regions of the mutant cortex. Values are presented as means ± SEMs (**0.001<P<0.01, ***P <0.001). Scale bar=100µm.

dcKO cortices had significantly high number of Sox2+/GLAST+ RGs in oSVZ compared to control (Fig. 11B). However, we also noticed that the number of Sox2+/GLAST+ cells in oSVZ are not statistically significantly different between BAF155cKO and dcKO mutants, although there is a tendency of increase in the latter (Fig. 11B).These data indicated that BAF155 and Pax6 synergistically maintain the pool of vRGs and modulate the genesis of bRGs.

Among its several key functions during cortical development, Pax6 plays an important role in RG cell division by regulating the mitotic cleavage plane (Asami et al., 2011). To find out whether BAF155 also has a similar role, we compared vRG mitotic cleavage planes between control, BAF155cKO, Pax6cKO and dcKO mutants by performing double IHC for pVim (cytoplasmic marker for dividing RGs) and pHH3 (nuclear marker for dividing cells) (Fig 11C). We found that loss of either Pax6 or BAF155 or both resulted in a shift in mitotic cleavage planes from vertical to orientations with reduced angle (Fig. 11D). It is particularly interesting to note that in the BAF155cKO cortex, there is a clear increase in the number of vRGs having horizontal cleavage plane orientation, which is known to predominantly generate bRGs (Asami et al., 2011; Estivill-Torrus et al., 2002). These findings indicate that both Pax6 and BAF155 have cell-autonomous roles in vRG cell division mode and genesis of BPs.

To further study the role of BAF155 and Pax6 in fate choice of vRGs, we carried out *in utero* electroporation (IUE) using Cre-ires-eGFP plasmid to delete either BAF155 or Pax6 from individual vRGs and their progenies in E13.5 cortex of BAF155fl/fl or Pax6fl/fl embryos (Fig. 12A-C). We collected tissues 30 hours after electroporation and immunostained for GFP, Sox2, Tbr2, (Postiglione et al., 2011; Tuoc et al., 2013). Statistical analysis revealed no significant difference in the number of GFP+/Sox2+ vRGs in Cre-injected BAF155fl/fl and control hemispheres (Fig. 5E/F). Contrastingly, the number of GFP+/Tbr2+ cells (IP fate) in SVZ was diminished in BAF155-ablated cortices as compared to control (Fig. 12A/B). As expected, the loss of BAF155 following IUE led to an obvious increase in the number of progenitors in oSVZ (Fig. 12A, white filled arrows) comprising of both GFP+/Sox2+ and GFP+/Tbr2+ cells (Fig. 12B/C). These outcomes support the idea that loss of BAF155 shifts the tendency of dividing vRGs to generate BPs in oSVZ rather than the generation of IPs in SVZ. Our IHC and statistical analysis also indicated that Pax6 loss of function (LOF) increased the magnitude of the above phenotypes that are observed in BAF155 LOF (Fig. 12A-C). It is interesting to note that, more GFP- basal progenitors (Fig. 12A, white empty arrows) than GFP+ (Fig. 12A, white filled arrows) were found in the oSVZ of Cre-injected BAF155fl/fl and Pax6fl/fl cortices (Fig. 12A-C). Taken together, our findings indicated that both BAF155 and Pax6 act in the same genetic pathway during cortical

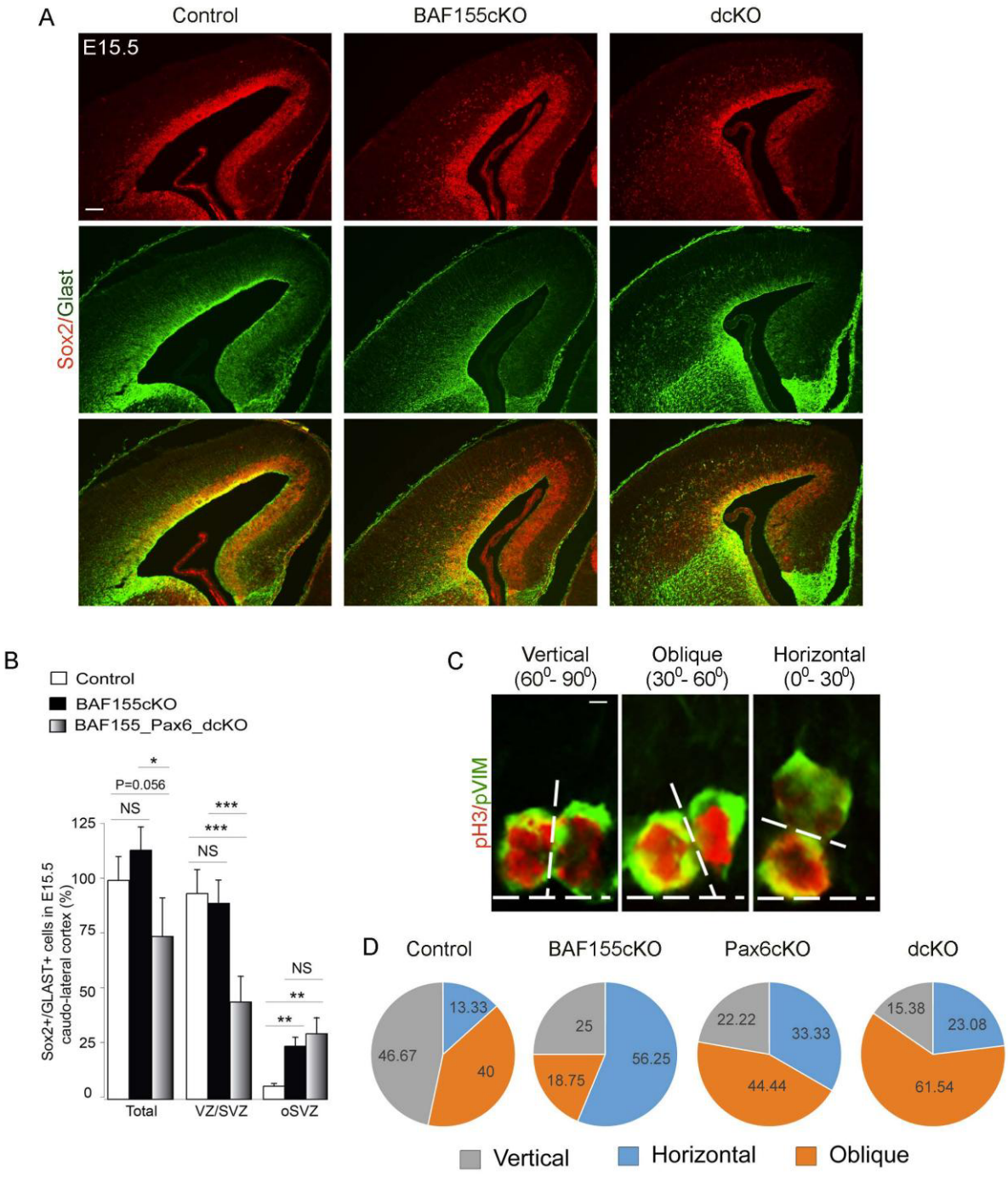

Figure 11. BAF155 and Pax6 has a cell-autonomous role in progenitor division and synergistically regulate genesis of basal progenitors

(A-B) IHC analysis using antibodies against nuclear (Sox2) and cytoplasmic (GLAST) RG marker in control, BAF155cKO and BAF155_Pax6_dcKO cortices at E15.5 (A). Loss of Pax6 in addition to BAF155 resulted in significant reduction in RG population in VZ, and a tendency towards increased basal RG population in oSVZ (B).

(C-D) To compare RG mitotic cleavage plane orientation in BAF155cKO, Pax6cKO and dcKO mutants, E15.5 cortices were stained for phosphorylated Vimentin (pVim) and phosphorylated Histone H3 (pHH3) to mark mitotic cells, and mitotic chromatin, respectively (C). The observed angle between the cleavage plane and the apical surface of the cortex were grouped into three classes, 60-90° scored as vertical, 30-60° as oblique and 0-30° as horizontal cell divisions. There is a shift from vertical to non-vertical divisions in the mutants, suggesting a cell-autonomous role for BAF155 and Pax6 in RG cell division (D). Scale bar=100µm.

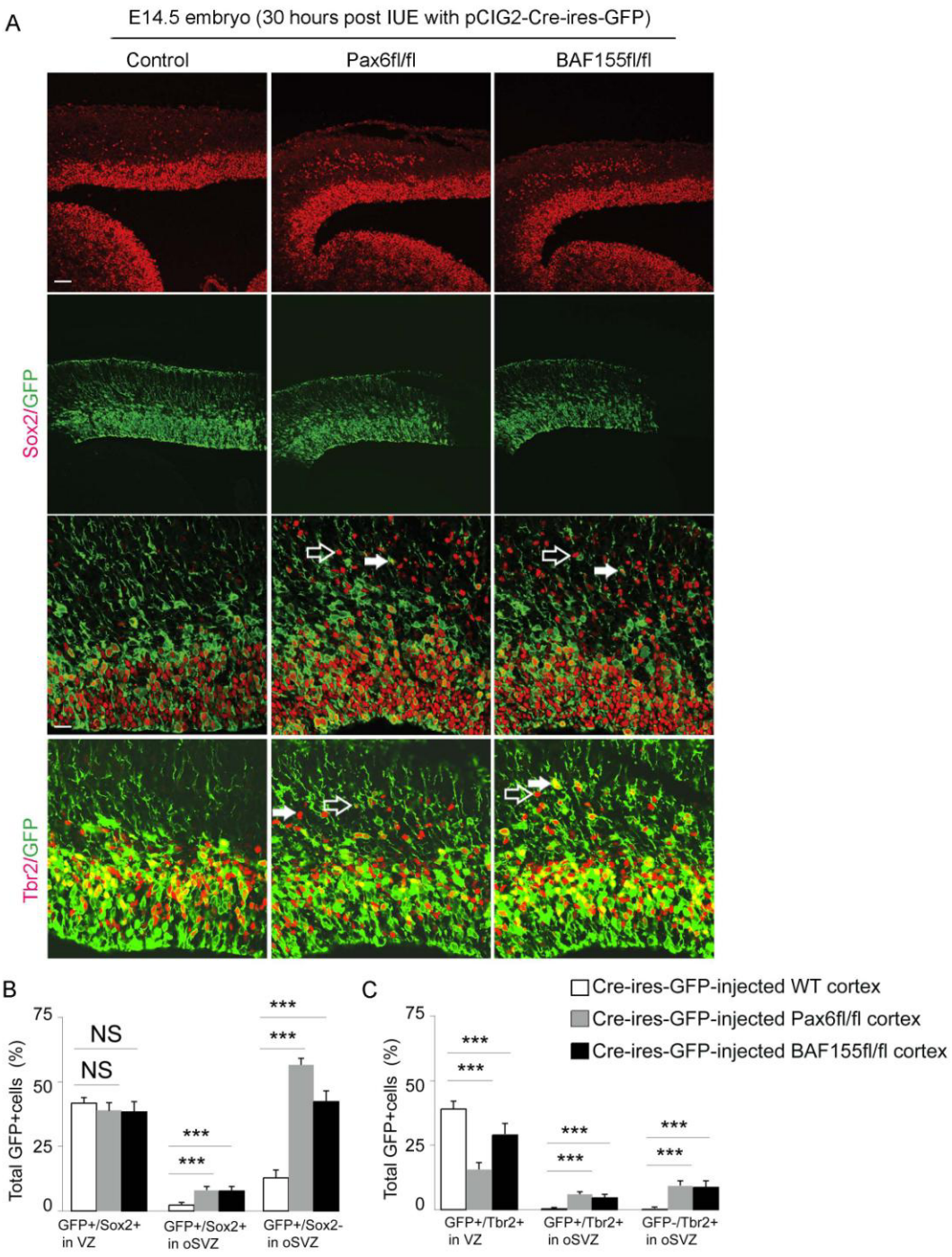

Figure 12. BAF155 and Pax6 control genesis of basal progenitors predominantly in non cell-autonomous manner

(A) E13.5 cortices of WT, Pax6fl/fl or BAF155fl/fl embryos were electroporated with Cre-eGFP. After 30 hours, sections of isolated brains were examined by IHC staining for expression of GFP, RG marker (Sox2), IPs (Tbr2) and images were acquired using fluorescence (upper panel) and confocal (lower panel) microscopes.

(B-C) Statistical analyses revealed that the loss of Pax6 and BAF155 in IUE experiments led to decrease in the number of GFP+/Tbr2+ IPs in SVZ, but not GFP+/Sox2+ RGs in VZ and increase in GFP+/Tbr2+ and GFP+/Sox2+ basal progenitors in oSVZ. Remarkably, the basal progenitors in oSVZ were predominantly GFP- (white empty arrows in A) than GFP+ (white filled arrows in A). Values are presented as means ± SEMs (***P <0.001). [Abbreviations: VZ, ventricular zone; SVZ, subventricular zone; oSVZ, outer subventricular zone]. Scale bar = 100µm.

development, so that the loss of BAF155 or Pax6 alters the cell division mode of vRGs, thereby producing BPs at the expense of IPs (cell-autonomous role). In addition to this, the loss of BAF155 or Pax6 in a subset of vRGs also leads to a significant increase in BPs that have originated from non-targeted vRGs possibly by delamination (non cell-autonomous role) from VZ.

BAF155 suppresses progenitor delamination by regulating adherens junction and cell-cell interaction machinery

Besides a cell-autonomous role in regulating BP genesis, we were intrigued by the finding that the loss of BAF155 or Pax6 causes significant delamination of progenitors from VZ. To further investigate this non cell-autonomous mechanism by which Pax6 and BAF155 control the genesis of BPs, we examined the genes most markedly down-regulated in Pax6cKO and BAF155cKO cortex that has particular relevance in the maintenance of VZ integrity. The GO analyses of the RNA-seq data showed a significant enrichment for genes involved in wide spectrum of cell-cell interaction and cell morphology, including cell-cell adherens junction, apical junction complex, basement membrane, actin cytoskeleton, regulation of cell shape and Rho protein signal transduction (Fig. 13A-C).

We then compared our RNA-seq data with the published Pax6-binding sites from ChIP-seq (Xie et al., 2013), ChIP-on-chip of Pax6 with cortical tissue (Sansom et al., 2009) and Brg1-binding sites from ChIP-seq with forebrain tissue (Attanasio et al., 2014) to identify possible direct target genes of Pax6 and BAF complexes that controls cell-cell interaction, adherens junction and thereby contributing to the genesis of BPs in non cell-autonomous manner (Fig. 13B/C). Promoter regions of candidate genes were cloned into vector driving luciferase expression and transiently transfected into Neuro2A cells together with a combination of CMV-Pax6 and shBAF155. Followed by lysate collection and luminescence quantification, our reporter assay confirmed that Pax6 directly binds and significantly regulates promoter activity of several genes that are crucial for cell-cell interaction (Luc+CMV-Pax6 condition) such as Pdgfrb, Ssx2ip, Fgfr1, Celsr2, Cdc42ep1 and Cdc42ep4 (Fig. 13D). The presence of BAF155 silencing vector tends to reduce this promoter activity (Luc+CMV-Pax6+shBAF155 condition), specifically in the case of Cdc42ep1 and Cdc42ep4 genes. For further studies, we focused on the two candidates: the CDC42 effector proteins 1 and 4 (Cdc42ep1/CEP1 and Cdc42ep4/CEP4), members of the Rho family of guanosine triphosphatases (GTPases), which are known to be key players in cytoskeletal remodeling and to act downstream of Cdc42 to induce actin filament organization that underlie cell shape dynamics (Hirsch et al., 2001; Joberty et al., 2001). Because CEP4, but not CEP1 is highly and restrictively expressed in E14.5 cortical VZ (Fig. 14A), we focused on understanding

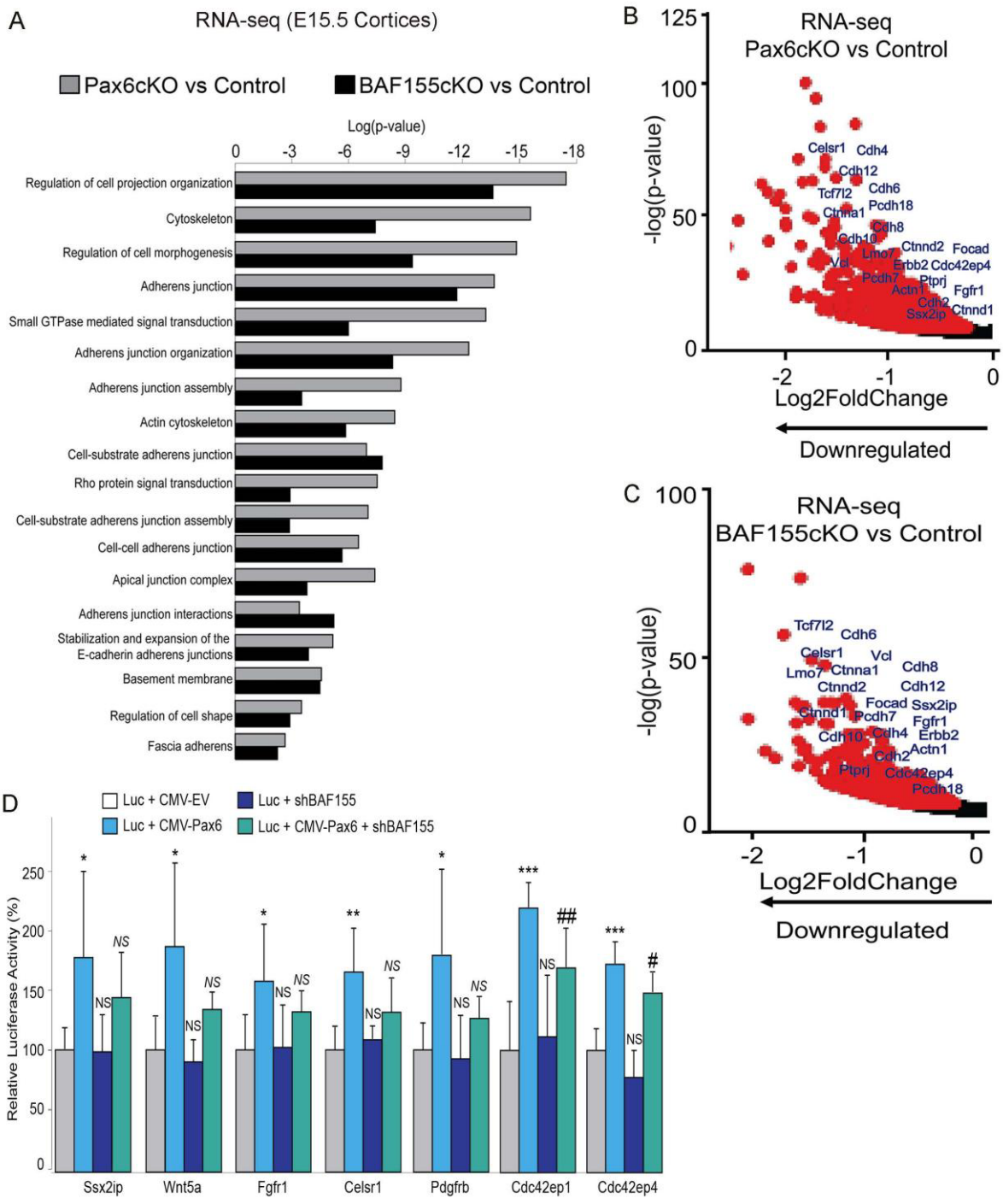

Figure 13. BAF155 and Pax6 regulates cell-cell interaction and adherens junction

(A) Analysis of gene ontology (GO) from RNA-seq data indicated that many gene pathways which are important for cell-cell interaction were altered in BAF155 and Pax6 mutants.

(B-C) RNA-Seq transcriptome profiling between control and Pax6cKO (B), BAF155cKO (C) cortices showing down-regulated transcripts, among which genes important for cell-cell interaction and cell-adhesion were highlighted in blue.

(D) Luciferase reporter assay revealed that Pax6 activates promoter activity of several Pax6-target genes that are crucial for cell-cell interaction (Luc+CMV-Pax6 condition). The presence of BAF155 silencing vector tends to reduce this promoter activity (Luc+CMV-Pax6+shBAF155 condition), specifically in the case of Cdc42ep1 and Cdc42ep4 genes.

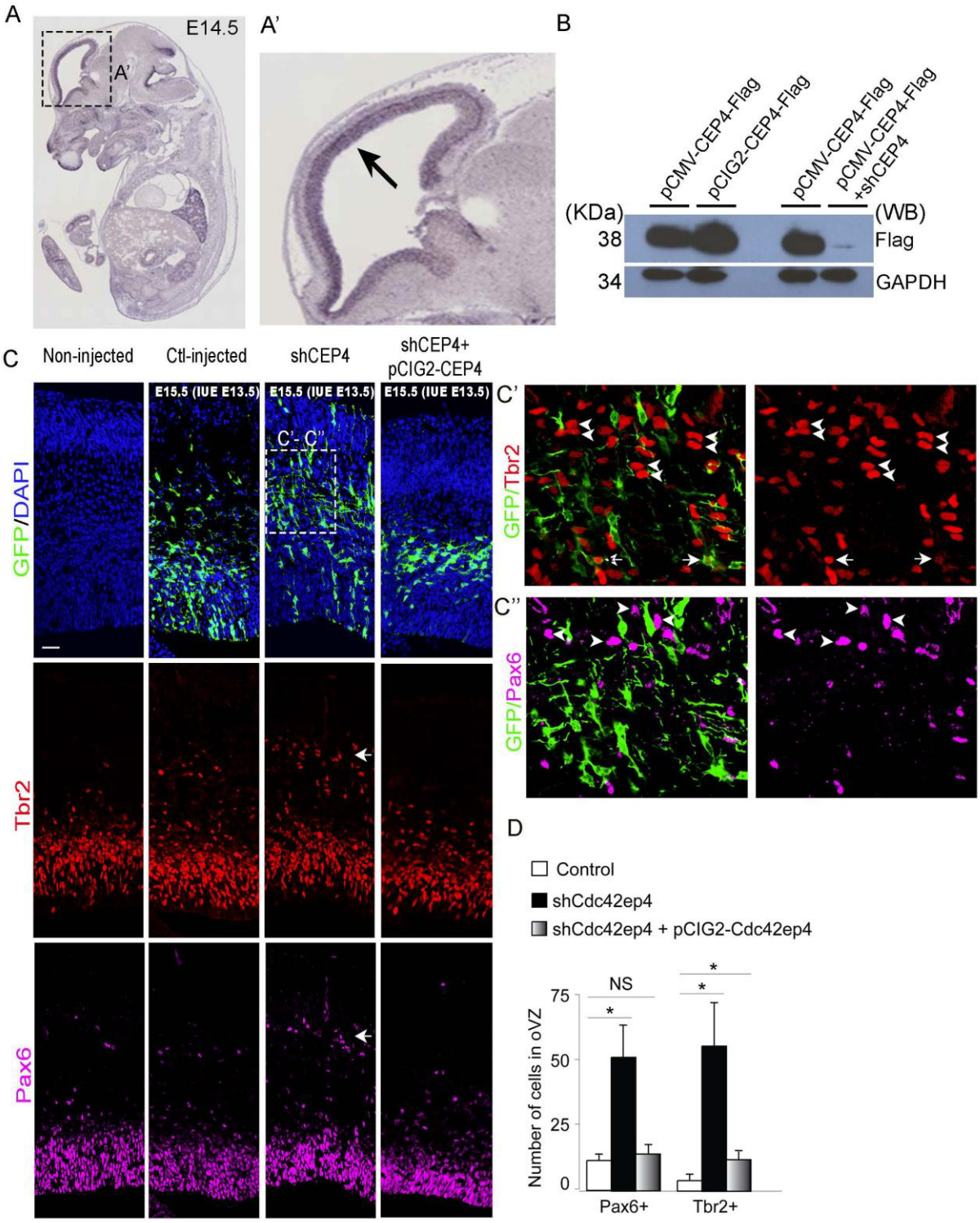

Figure 14. BAF155 regulates non cell-autonomous generation of basal progenitors through a novel Pax6-dependent mechanism mediated by CEP4

Figure 14. BAF155 regulates non cell-autonomous generation of basal progenitors through a novel Pax6-dependent mechanism mediated by CEP4

(A) *In situ* hybridization for CEP4 in sagittal section of E14 mouse embryo from GenePaint database. Higher magnification of the cortex (A') shows ventricular zone-specific localization of CEP4 transcripts. (B) HEK293T cells were transiently transfected with the respective flag-tagged plasmid(s) and cell lysates collected after 48 hours for western blotting (GAPDH used as a loading control). In the first two lanes, expression levels of the CMV- and pCIG2-CEP4 plasmids were tested and in the last two lanes, the efficiency of short hairpin construct against CEP4 was tested. (C) E13.5 wildtype cortices were electroporated with either control or CEP4 silencing vectors. After 48 hrs, loss of function of CEP4 lead to significant delamination of progenitors generating both bRGs and bIPs in the oSVZ. Interestingly, the majority of these basal progenitors were GFP- (white arrow heads in C'/C'') than GFP+ (white arrows in C'/C''). Combining CEP4 silencing vector and CEP4 expression vector resulted in fewer basal progenitors thus rescuing the phenotype. (D) Statistical analysis of the number of Pax6+ and Tbr2+ progenitors in oSVZ in the above experiment revealed that there is a significant increase in basal progenitors upon CEP4 silencing compared to control electroporated cortex. In addition, the coexpression of CEP4 rescued this phenotype. Values are presented as means ± SEMs (*0.01<P<0.05). [Abbreviations: bRG, basal radial glia; bIP, basal intermediate progenitor; oSVZ, outer subventricular zone]. Scale bar = 100μm.

whether CEP4 is important for genesis of BPs. To ascertain this, we designed a short hairpin RNA (shRNA) construct against CEP4 (Fig. 14B) and electroporated it into E13.5 WT cerebral cortices (Fig. 14C). Strikingly, two days post-electroporation, the effect of silencing CEP4 was evidenced by a dramatic increase in numbers of both Pax6+ bRGs and Tbr2+ bIPs compared to the cortex electroporated with the control vector (Fig. 14C/D). Notably, similar to loss of BAF155 and Pax6, majority of bIPs and bRGs in CEP4 shRNA electroporated cortex is negative for GFP (Fig. 14C'/C''), which is consistent with a role of CEP4 in the organization of the actin cytoskeleton and cell-cell interaction (Hirsch et al., 2001; Joberty et al., 2001). Co-transfection of CEP4 shRNA and pCIG2-CEP4 overexpression plasmid was able to rescue the effect of CEP4 silencing (Fig. 14C/D). Taken together, these findings strongly support the idea that Pax6 and BAF155 control genesis of bRGs and bIPs in non cell-autonomous manner, at least in part by directly regulating target genes involved in cell shape dynamics and cell-cell interaction such as CEP4.

BAF155 regulates the expression of novel human RG specific genes in a Pax6-independent manner

In the recent years, several studies focused on the key differences between mouse and human RG cell (hRGs) population and have successfully identified several novel genes that are exclusively expressed in hRGs (Lui et al., 2014). Since our BAF155cKO consists of a distinct population of BPs at the oSVZ which is normally not found in a wildtype mouse cortex, we were interested to compare our RNA-seq data with that from other published studies. Surprisingly, transcript levels of three hRG specific genes, namely Foxn4, Lrig3 and C8orf4, were upregulated in BAF155cKO but not in Pax6cKO cortex. Among these, we found Foxn4 to be particularly interesting because despite its presence in

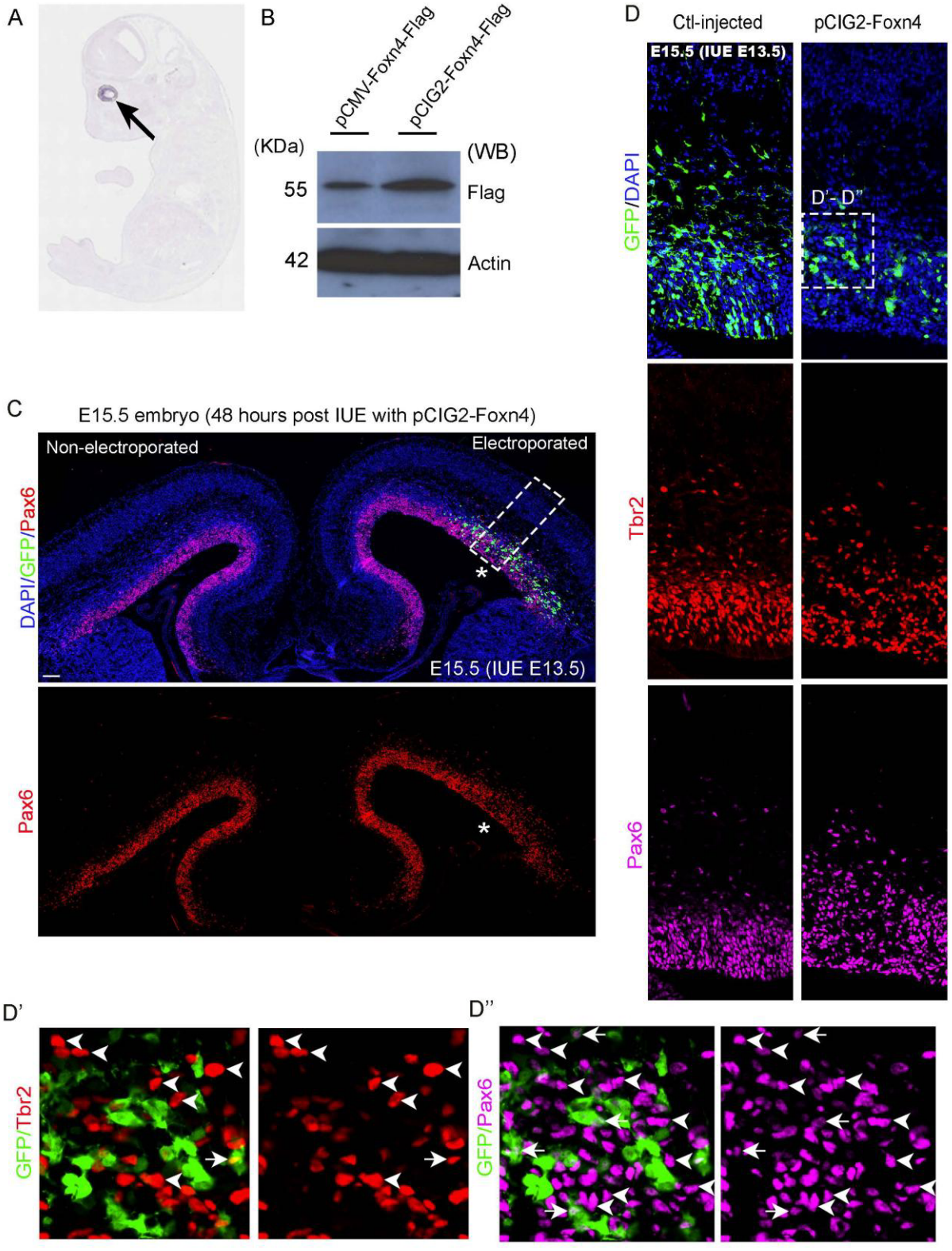

Figure 15. BAF155 regulates non cell-autonomous generation of basal progenitors through a novel Pax6-independent mechanism mediated by Foxn4

Figure 15. BAF155 regulates non cell-autonomous generation of basal progenitors through a novel Pax6-independent mechanism mediated by Foxn4

(A) *In situ* hybridization for Foxn4 in sagittal section of E14 mouse embryo from GenePaint database shows retina-specific localization of Foxn4 transcripts and their absence in cortex.

(B) HEK293T cells were transiently transfected with the respective flag-tagged plasmid(s) and cell lysates collected after 48 hours for western blotting (Actin used as a loading control). First lane depicts expression levels of the CMV-Foxn4 plasmid and the second, pCIG2-Foxn4 plasmid which was used for IUE.

(C) E13.5 wildtype cortex electroporated with Foxn4 expression vector resulted in massive delamination of Pax6+ RG after 48 hrs compared to non-electroporated hemisphere.

(D) High magnification confocal image of the region highlighted by white frame in C shows that the gain of function of Foxn4 lead to significant delamination of progenitors generating abundant bRGs and bIPs in the oSVZ. Interestingly, the majority of these basal progenitors were GFP- (white arrow heads in D'/D'') than GFP+ (white arrows in D'/D''). Scale bar=100μm.

the mouse genome, it is not expressed in the mouse cortex (Fig. 15A). In order to further characterize the possible roles of Foxn4 in cortical development, we decided to perform Foxn4 gain of function (GOF) in WT cortex. To this end, we created an expression vector having Foxn4 cDNA under pCIG2 promoter (Fig. 15B) and electroporated it into E13.5 WT cerebral cortices. Two days post-electroporation, we observed massive delamination of both Pax6+ RGs and Tbr2+ IPs, giving rise to abundant BPs (Fig. 15C/D). Interestingly, majority of the BPs were GFP- (Fig. 15D'/D''), strikingly similar to the phenotype observed with LOF of BAF155 and CEP4. These results indicated that during mouse cortical development, BAF155 suppresses the expression of novel hRG-specific genes such as Foxn4 which otherwise promotes abundant generation of BPs.

Discussion

During cerebral cortex development, glutamatergic neurons are produced in an inside-out fashion such that the lower layer (LL) neurons precede the upper layer (UL) neurons. Through different modes of neurogenesis, vRGs either give rise to LL neurons (direct neurogenesis) or to UL neurons (indirect neurogenesis) through their descendent BPs residing in the SVZ. The pool of BPs have evolved greatly during mammalian evolution. In the case of lissencephalic species like rodents, the SVZ is mainly populated by IPs which predominantly accounts for the generation of UL neurons, thereby resulting in the radial expansion of the cortex. However, in gyrencephalic species like primates and humans, the pool of BPs is much expanded comprising not only of IPs in the iSVZ (similar to rodents), but also bRGs and bIPs forming the oSVZ, resulting in an exponential increase in neuronal output that underlies greater expansion and folding of the cortex. In this study, we have elucidated a novel mechanism by which the BAF155 subunit of chromatin remodelling BAF complex regulates BP genesis through a Pax6-dependent and independent mechanism.

BAF155 regulates fate choice of apical progenitors to promote IP genesis similar to Pax6

Besides its role in telencephalon patterning, Pax6 is a RG-specific transcription factor that determines vRG fate and subsequent IP generation (Georgala et al., 2011; Gotz et al., 1998; Quinn et al., 2006; Sansom et al., 2009; Tuoc et al., 2009). Specifically, during asymmetric vRG division, Pax6 activates the expression of genes such as Tbr2 leading to the commitment of the progeny to IP fate and the loss of Tbr2 causes severe reduction of IPs (Arnold et al., 2008; Sessa et al., 2008). In this study, using a cerebral cortex-specific conditional inactivation system (Emx1-Cre) for BAF155, we found that BAF155cKO mice displayed similar phenotypic features when compared to Pax6cKO, including diminished pool of IPs. Our reporter assay revealed that BAF155 is needed for activating Pax6-dependent transcription in cortical progenitors. In addition, the RNA sequencing of BAF155cKO and Pax6cKO cortices revealed a significant overlap among genes that are either up- or down-regulated in both, including those involved in specifying IP fate. Therefore, our findings indicated a link between BAF155-dependent chromatin changes and Pax6-dependent transcriptional program that controls IP genesis during cortical development.

BAF155 and Pax6 promotes adherens junction formation and VZ integrity

In addition to reduced IP pool, the loss of Pax6 is known to trigger detachment of vRGs from apical surface due to overall reduction in cell adhesion proteins (Asami et al., 2011; Stoykova et al., 1997). Interestingly, there is also an increased frequency of progenitor delamination from VZ in the

BAF155cKO cortex, which is also reflected in our RNA sequencing data showing significant down-regulation of adherens junction (AJ)-specific genes. This highlighted the role of both BAF155 and Pax6 in AJ formation to anchor vRGs in the VZ.

BAF155 and Pax6 regulates bRG genesis through a novel CEP4-dependent non cell-autonomous mechanism

Consistent with the role of Pax6 in regulating the mode of cell division in vRGs (Asami et al., 2011), we also found that the loss of BAF155 causes more frequent horizontal cleavage plane orientations in vRGs, indicating its cell-autonomous role in bRG genesis. However, an important finding in this study is that the majority of BPs found both in the BAF155 and Pax6 LOF cortices arise through non-cell autonomous mechanism. In order to gain further mechanistic insights, taking clues from our RNA sequencing analysis, we identified CEP4, a Cdc42 effector protein, which is expressed exclusively at the VZ during mouse cortical development and down-regulated upon loss of BAF155 and Pax6. Being a multifaceted regulator of cellular processes, Rho GTPase Cdc42 has a documented role in the maintenance of vRG apico-basal polarity and AJ in the cortex (Cappello et al., 2006). Despite the identification of a family of Cdc42 effector proteins, their specific role during cortical development remains unknown. Our reporter assay revealed that BAF155 directly regulates the expression of CEP4 in a Pax6-dependent manner and that the loss of function of CEP4 causes delamination of progenitors in a predominantly non-cell autonomous manner. Therefore, in this study, we have identified a novel mechanism by which BAF155, specifically through its modulation of the Rho GTPase CEP4, balances VZ integrity and BP genesis. Our findings suggest that CEP4 might in part mediate the previously described role of Cdc42 in regulating apical progenitor fate and cortical development.

BAF155 specifies a restricted period during early cortical development that promotes progenitor delamination

Earlier studies showed that targeted deletion of Pax6 in vRGs resulted in the generation of basal progenitors maintaining characteristics of radial glia (Asami et al., 2011) and on the other hand, sustained expression of Pax6 in mouse vRGs that were fated to produce basal progenies, also resulted in the generation of primate-like bRGs (Wong et al., 2015). These findings suggested a dual role for Pax6 in regulating the fate of vRGs and the resultant progenies. Since our findings established that BAF155 is required for Pax6-dependent transcriptional activity, it is plausible that such a dual role is achieved through spatial and temporal activation/repression of Pax6-dependent gene expression

during cortical development. A recent study reported that the pioneer bRG population in oSVZ is generated by delamination of vRGs during a restricted period in early cortical development in ferrets. Notably, the study also showed that such a period is delineated by a substantial reduction in Cdh1, Trnp1 expression, alongside change in the orientation of mitotic division plane (Martinez-Martinez et al., 2016). Interestingly, we found that BAF155 is expressed at very low levels in vRGs during early corticogenesis and the conditional inactivation of BAF155 in late cortical progenitors failed to generate BPs. These results indicated that the temporal expression pattern of BAF155 plausibly have functional relevance for vRG delamination and resultant BP genesis during cortical development, likely through its Pax6-dependent regulation of genes crucial for vRG anchoring, such as CEP4.

Non cell-autonomous mechanism of progenitor delamination mediated by BAF155 might be a hallmark of cortical evolution

Given the exponential increase in BPs and an expanded oSVZ in primate and human cortex, it is interesting to study whether such non-cell autonomous mechanism of progenitor delamination has acquired evolutionary significance in the process of BP genesis. In an attempt to identify novel factors that may underlie the unique phenotype observed in the BAF155cKO cortex, we compared our RNA sequencing results with that of other studies performed in mouse and human RG cell populations (Lui et al., 2014). Interestingly, loss of BAF155 resulted in the upregulation of transcripts of three genes, Foxn4, Lrig3 and C8orf4 which were previously identified as novel hRG-specific markers that are absent in mouse RGs (Lui et al., 2014). Among these genes, Foxn4 was particularly interesting to us due to its specific expression in mouse retina and as a regulator of retinal progenitor cell fate and neurogenesis (Li et al., 2004). To further characterize the role of Foxn4 in the context of BP genesis, we performed a gain of function study. To our surprise, the overexpression of Foxn4 in the mouse cortex resulted in massive progenitor delamination and abundant generation of both bRGs and bIPs. Consistent with the CEP4 LOF experiment, the majority of these BPs are generated in non-cell autonomous manner. Notably, the GOF of Foxn4 displayed a strikingly similar phenotype that was previously reported for the GOF of PDGFRb, another novel hRG-specific marker (Lui et al., 2014). These results indicated that besides a Pax6-dependent role, BAF155 also regulates BP genesis independently albeit through a similar non-cell autonomous mechanism.

In summary, findings in this study revealed the significance of the interaction between the chromatin remodeling BAF complex and transcriptional machinery in the context of apical progenitor fate choice and basal progenitor genesis during cortical development. Specifically, this study highlighted the role

of BAF155 and Pax6 in AJ formation to anchor vRGs in the VZ. However, during a restricted period in early corticogenesis, the absence of BAF155 promotes progenitor delamination resulting in the generation of bRGs, which sequentially express molecular markers characteristic of progenitor differentiation forming a distinct oSVZ similar to that in gyrencephalic cortex. In addition, the findings in this study suggested that besides cell-autonomous role of BAF155 and Pax6 in apical progenitors, there exists novel cell-cell interaction machinery that operates at the population-wide level to bring about significant changes in cortical development. We have elucidated such a mechanism in which BAF155 and Pax6 directly regulates CEP4, a Cdc42 effector protein that has a novel role in progenitor delamination. Interestingly, through the regulation of novel hRG-specific genes such as Foxn4, BAF155 also has Pax6-independent role in delamination and bRG genesis. This study also suggests that such non-cell autonomous mechanisms of BP genesis might have acquired evolutionary significance during cortical development.

Summary

During mammalian development, the balance between symmetric and asymmetric division of radial glial (RG) progenitors regulates the tangential size versus radial growth of the cerebral cortex. The pool of basal progenitors (BPs) that contribute to radial growth have expanded greatly during evolution and studies in the past have identified several underlying key transcriptional and signalling mechanisms. In this study, we found that the interaction between BAF155 subunit of the mSWI/SNF chromatin-remodeling complex and Pax6, a key transcriptional regulator of corticogenesis, controls the fate choice of mouse RG specifically during early cortical development. Besides a cell-autonomous role in regulating RG division, we also found that the loss of BAF155 and Pax6 causes delamination of RG from the VZ to generate basal RG, through a novel CEP4 dependent non cell-autonomous mechanism. Interestingly, our results also suggested that such a non cell-autonomous mechanism of BP genesis might be a hallmark of primate cortical development.

Abbreviations

AJ	Adherens junction
BAF	Brg1/Brm associated factor
bIPs	Basal Intermediate Progenitors
BLBP	Brain lipid binding protein
BPs	Basal progenitors
bRGs	Basal radial glial cells
C8orf4	Chromosome 8 open reading frame
Cdc42	Cell division cycle 42
Cdc42ep1	Cdc42 effector protein 1
Cdc42ep4	Cdc42 effector protein 4
Cdh1	Cadherin 1
cDNA	Complementary deoxyribonucleic acid
CEP4	Cdc42ep4
ChIP-seq	Chromatin immunoprecipitation sequencing
cKO	Conditional knockout
CP	Cortical plate
DAPI	4,6-dasmindino-2-phenylindol
dcKO	Double conditional knockout
DIV	Days *in vitro*
DMEM	Dulbecco's Modified Eagle Medium
DNA	Deoxyribonucleic acid
E	Embryonic day
eGFP	Enhanced green fluorescent protein
Emx1	Empty spiracles homeobox 1
Fgfr1	Fetal growth factor 1
Fl	Floxed
Foxn4	Forkhead box n4
GFP	Green fluorescent protein
GLAST	GLutamate Aspartate Transporter
GO	Gene ontology

GOF	Gain of function
GTPases	Guanosine tri-phosphatases
h	hours
hGFAP	Human glial fibrillary acidic protein
hRGs	Human radial glial cells
HRP	Horseradish-peroxidase
IHC	Immune histochemistry
IPs	Intermediate progenitor cells
Ires	Internal ribosomal entry site
iSVZ	Inner sub-ventricular zone
IUE	In utero electroporation
IZ	Intermediate zone
LL	Lower layer
LOF	Loss of function
Luc	Luciferase
MRI	Magnetic resonance imaging
Ngn2	Neurogenin 2
NSC	Neural stem cell
oSVZ	Outer sub-ventricular zone
P	Postnatal stage
Pax6	Paired box 6
PBS	Phosphate Buffer Saline
PCR	Polymerase chain reaction
Pdgfrb	Platelet derived growth factor b
PFA	Paraformaldehyde
pHH3	Phosphorylated histone 3
PVim	Phosphorylated vimentin
RGs	Radial glial cells
rpm	Revolutions per minute
RT	Room temperature
RNA-seq	Ribonucleic acid sequencing
SDS	Sodium dodecyl sulphate

sh	Short hairpin
Sox2	SRY- related HMG transcription factor 2
SVZ	Sub-ventricular zone
Tbr1	T-box brain 1
Tbr2	T-box brain 2
TE	Tris EDTA
TF	Transcription factor
UL	Upper layer
vRGs	Ventricular radial glial cells
VZ	ventricular zone
WB	Western blot
WT	wildtype

References

Arnold, S.J., Huang, G.J., Cheung, A.F., Era, T., Nishikawa, S., Bikoff, E.K., Molnar, Z., Robertson, E.J., and Groszer, M. (2008). The T-box transcription factor Eomes/Tbr2 regulates neurogenesis in the cortical subventricular zone. Genes Dev 22, 2479-2484.

Asami, M., Pilz, G.A., Ninkovic, J., Godinho, L., Schroeder, T., Huttner, W.B., and Gotz, M. (2011). The role of Pax6 in regulating the orientation and mode of cell division of progenitors in the mouse cerebral cortex. Development 138, 5067-5078.

Ashery-Padan, R., Marquardt, T., Zhou, X., and Gruss, P. (2000). Pax6 activity in the lens primordium is required for lens formation and for correct placement of a single retina in the eye. Genes Dev 14, 2701-2711.

Attanasio, C., Nord, A.S., Zhu, Y., Blow, M.J., Biddie, S.C., Mendenhall, E.M., Dixon, J., Wright, C., Hosseini, R., Akiyama, J.A., et al. (2014). Tissue-specific SMARCA4 binding at active and repressed regulatory elements during embryogenesis. Genome research 24, 920-929.

Betizeau, M., Cortay, V., Patti, D., Pfister, S., Gautier, E., Bellemin-Menard, A., Afanassieff, M., Huissoud, C., Douglas, R.J., Kennedy, H., et al. (2013). Precursor diversity and complexity of lineage relationships in the outer subventricular zone of the primate. Neuron 80, 442-457.

Cappello, S., Attardo, A., Wu, X., Iwasato, T., Itohara, S., Wilsch-Brauninger, M., Eilken, H.M., Rieger, M.A., Schroeder, T.T., Huttner, W.B., et al. (2006). The Rho-GTPase cdc42 regulates neural progenitor fate at the apical surface. Nat Neurosci 9, 1099-1107.

Chen, J., Bardes, E.E., Aronow, B.J., and Jegga, A.G. (2009). ToppGene Suite for gene list enrichment analysis and candidate gene prioritization. Nucleic acids research 37, W305-311.

Choi, B.H., and Lapham, L.W. (1978). Radial glia in the human fetal cerebrum: a combined Golgi, immunofluorescent and electron microscopic study. Dev Brain Res 148, 295–311.

Choi, J., Ko, M., Jeon, S., Jeon, Y., Park, K., Lee, C., Lee, H., and Seong, R.H. (2012). The SWI/SNF-like BAF complex is essential for early B cell development. Journal of immunology 188, 3791-3803.

Dehay, C., and Kennedy, H. (2007). Cell-cycle control and cortical development. Nat Rev Neurosci 8, 438-450.

Epstein, J., Cai, J., Glaser, T., Jepeal, L., and Maas, R. (1994). Identification of a Pax paired domain recognition sequence and evidence for DNA-dependent conformational changes. J Biol Chem 269, 8355-8361.

Estivill-Torrus, G., Pearson, H., van Heyningen, V., Price, D.J., and Rashbass, P. (2002). Pax6 is required to regulate the cell cycle and the rate of progression from symmetrical to asymmetrical division in mammalian cortical progenitors. Development 129, 455-466.

Farkas, L.M., and Huttner, W.B. (2008). The cell biology of neural stem and progenitor cells and its significance for their proliferation versus differentiation during mammalian brain development. Curr Opin Cell Biol 20, 707-715.

Feng, L., Hatten, M.E., and Heintz, N. (1994). Brain lipid-binding protein (BLBP): a novel signaling system in the developing mammalian CNS. Neuron 12, 895-908.

Fietz, S. A., I. Kelava, et al. (2010). OSVZ progenitors of human and ferret neocortex are epithelial-like and expand by integrin signaling. Nature neuroscience 13(6): 690-699.

Fish, J.L., Dehay, C., Kennedy, H., and Huttner, W.B. (2008). Making bigger brains-the evolution of neural-progenitor-cell division. J Cell Sci 121, 2783-2793.

Gadisseux, J.F., Kadhim, H.J., van den Bosch de Aguilar, P., Caviness, V.S., and Evrard, P. (1990). Neuron migration within the radial glial fiber system of the developing murine cerebrum: an electron microscopic autoradiographic analysis. Brain Res Dev Brain Res 52, 39-56.

Georgala, P.A., Manuel, M., and Price, D.J. (2011). The generation of superficial cortical layers is regulated by levels of the transcription factor Pax6. Cerebral cortex 21, 81-94.

Goebbels, S., Bormuth, I., Bode, U., Hermanson, O., Schwab, M.H., and Nave, K.A. (2006). Genetic targeting of principal neurons in neocortex and hippocampus of NEX-Cre mice. Genesis 44, 611-621.

Gorski, J.A., Talley, T., Qiu, M., Puelles, L., Rubenstein, J.L., and Jones, K.R. (2002). Cortical excitatory neurons and glia, but not GABAergic neurons, are produced in the Emx1-expressing lineage. J Neurosci 22, 6309-6314.

Gotz, M., and Huttner, W.B. (2005). The cell biology of neurogenesis. Nat Rev Mol Cell Biol 6, 777-788.

Gotz, M., Stoykova, A., and Gruss, P. (1998). Pax6 controls radial glia differentiation in the cerebral cortex. Neuron 21, 1031-1044.

Guillemot, F. (2007). Cell fate specification in the mammalian telencephalon. Prog Neurobiol 83, 37-52.

Hansen, D.V., Lui, J.H., Parker, P.R., and Kriegstein, A.R. (2010). Neurogenic radial glia in the outer subventricular zone of human neocortex. Nature 464, 554-561.

Hatten, M.E., and Mason, C.A. (1990). Mechanisms of glial-guided neuronal migration in vitro and in vivo. Experientia 46, 907-916.

Haubensak, W., Attardo, A., Denk, W., and Huttner, W.B. (2004). Neurons arise in the basal neuroepithelium of the early mammalian telencephalon: a major site of neurogenesis. Proc Natl Acad Sci U S A 101, 3196-3201. Epub 2004 Feb 3112.

Hevner, R.F., Hodge, R.D., Daza, R.A., and Englund, C. (2006). Transcription factors in glutamatergic neurogenesis: conserved programs in neocortex, cerebellum, and adult hippocampus. Neurosci Res 55, 223-233.

Hirsch, D.S., Pirone, D.M., and Burbelo, P.D. (2001). A new family of Cdc42 effector proteins, CEPs, function in fibroblast and epithelial cell shape changes. The Journal of biological chemistry 276, 875-883.

Hsieh, J., and Gage, F.H. (2005). Chromatin remodeling in neural development and plasticity. Curr Opin Cell Biol 17, 664-671.

Joberty, G., Perlungher, R.R., Sheffield, P.J., Kinoshita, M., Noda, M., Haystead, T., and Macara, I.G. (2001). Borg proteins control septin organization and are negatively regulated by Cdc42. Nature cell biology 3, 861-866.

Kriegstein, A., Noctor, S., and Martinez-Cerdeno, V. (2006). Patterns of neural stem and progenitor cell division may underlie evolutionary cortical expansion. Nat Rev Neurosci 7, 883-890.

Leone, D.P., Srinivasan, K., Chen, B., Alcamo, E., and McConnell, S.K. (2008). The determination of projection neuron identity in the developing cerebral cortex. Curr Opin Neurobiol 18, 28-35.

Levitt, P., Cooper, M.L., and Rakic, P. (1983). Early divergence and changing proportions of neuronal and glial precursor cells in the primate cerebral ventricular zone. Dev Biol 96.

Li, S., Mo, Z., Yang, X., Price, S.M., Shen, M.M., and Xiang, M. (2004). Foxn4 controls the genesis of amacrine and horizontal cells by retinal progenitors. Neuron 43, 795-807.

Love, M.I., Huber, W., and Anders, S. (2014). Moderated estimation of fold change and dispersion for RNA-seq data with DESeq2. Genome biology 15, 1.

Lui, J.H., Hansen, D.V., and Kriegstein, A.R. (2011). Development and evolution of the human neocortex. Cell 146, 18-36.

Lui, J.H., Nowakowski, T.J., Pollen, A.A., Javaherian, A., Kriegstein, A.R., and Oldham, M.C. (2014). Radial glia require PDGFD-PDGFRbeta signalling in human but not mouse neocortex. Nature 515, 264-268.

Malatesta, P., Hartfuss, E., and Gotz, M. (2000). Isolation of radial glial cells by fluorescent-activated cell sorting reveals a neuronal lineage. Development 127, 5253-5263.

Martinez-Cerdeno, V., Cunningham, C.L., Camacho, J., Antczak, J.L., Prakash, A.N., Cziep, M.E., Walker, A.I., and Noctor, S.C. (2012). Comparative analysis of the subventricular zone in rat, ferret and macaque: evidence for an outer subventricular zone in rodents. PLoS One 7, e30178.

Martinez-Martinez, M.A., De Juan Romero, C., Fernandez, V., Cardenas, A., Gotz, M., and Borrell, V. (2016). A restricted period for formation of outer subventricular zone defined by Cdh1 and Trnp1 levels. Nat Commun 7, 11812.

Misson, J.-P., Takahashi, T., and Caviness, V.S., Jr. (1991). Ontogeny of radial and other astroglial cells in murine cerebral cortex. Glia 4, 138–148.

Miyata, T. (2007). Asymmetric cell division during brain morphogenesis. Prog Mol Subcell Biol 45, 121-142.

Miyata, T., Kawaguchi, A., Saito, K., Kawano, M., Muto, T., and Ogawa, M. (2004). Asymmetric production of surface-dividing and non-surface-dividing cortical progenitor cells. Development 131, 3133-3145.

Molnar, Z., Metin, C., Stoykova, A., Tarabykin, V., Price, D.J., Francis, F., Meyer, G., Dehay, C., and Kennedy, H. (2006). Comparative aspects of cerebral cortical development. Eur J Neurosci 23, 921-934.

Molyneaux, B.J., Arlotta, P., Menezes, J.R., and Macklis, J.D. (2007). Neuronal subtype specification in the cerebral cortex. Nat Rev Neurosci 8, 427-437.

Narayanan, R., Pirouz, M., Kerimoglu, C., Pham, L., Wagener, R.J., Kiszka, K.A., Rosenbusch, J., Seong, R.H., Kessel, M., Fischer, A., et al. (2015). Loss of BAF (mSWI/SNF) Complexes Causes Global Transcriptional and Chromatin State Changes in Forebrain Development. Cell Rep 13, 1842-1854.

Noctor, S.C., Martinez-Cerdeno, V., Ivic, L., and Kriegstein, A.R. (2004). Cortical neurons arise in symmetric and asymmetric division zones and migrate through specific phases. Nat Neurosci 7, 136-144.

O'Leary, D.D., Chou, S.J., and Sahara, S. (2007). Area patterning of the mammalian cortex. Neuron 56, 252-269.

Ochiai, W., Nakatani, S., Takahara, T., Kainuma, M., Masaoka, M., Minobe, S., Namihira, M., Nakashima, K., Sakakibara, A., Ogawa, M., et al. (2009). Periventricular notch activation and asymmetric Ngn2 and Tbr2 expression in pair-generated neocortical daughter cells. Mol Cell Neurosci 40, 225-233.

Pinto, L., Drechsel, D., Schmid, M.T., Ninkovic, J., Irmler, M., Brill, M.S., Restani, L., Gianfranceschi, L., Cerri, C., Weber, S.N., et al. (2009). AP2gamma regulates basal progenitor fate in a region- and layer-specific manner in the developing cortex. Nat Neurosci 12, 1229-1237.

Pontious, A., Kowalczyk, T., Englund, C., and Hevner, R.F. (2008). Role of intermediate progenitor cells in cerebral cortex development. Dev Neurosci 30, 24-32.

Postiglione, M.P., Juschke, C., Xie, Y., Haas, G.A., Charalambous, C., and Knoblich, J.A. (2011). Mouse inscuteable induces apical-Basal spindle orientation to facilitate intermediate progenitor generation in the developing neocortex. Neuron 72, 269-284.

Quinn, J.C., Molinek, M., Martynoga, B.S., Zaki, P.A., Faedo, A., Bulfone, A., Hevner, R.F., West, J.D., and Price, D.J. (2006). Pax6 controls cerebral cortical cell number by regulating exit from the cell cycle and specifies cortical cell identity by a cell autonomous mechanism. Dev Biol 22, 22.

Rakic, P. (1972). Mode of cell migration to the superficial layers of fetal monkey neocortex. J Comp Neurol 145, 61-83.

Rakic, P. (2009). Evolution of the neocortex: a perspective from developmental biology. Nat Rev Neurosci 10, 724-735.

Sansom, S.N., Griffiths, D.S., Faedo, A., Kleinjan, D.J., Ruan, Y., Smith, J., van Heyningen, V., Rubenstein, J.L., and Livesey, F.J. (2009). The level of the transcription factor Pax6 is essential for controlling the balance between neural stem cell self-renewal and neurogenesis. PLoS Genet 5, e1000511.

Sessa, A., Mao, C.A., Hadjantonakis, A.K., Klein, W.H., and Broccoli, V. (2008). Tbr2 directs conversion of radial glia into basal precursors and guides neuronal amplification by indirect neurogenesis in the developing neocortex. Neuron 60, 56-69.

Shibata, T., Yamada, K., Watanabe, M., Ikenaka, K., Wada, K., Tanaka, K., and Inoue, Y. (1997). Glutamate transporter GLAST is expressed in the radial glia-astrocyte lineage of developing mouse spinal cord. J Neurosci 17, 9212-9219.

Stoykova, A., Gotz, M., Gruss, P., and Price, J. (1997). Pax6-dependent regulation of adhesive patterning, R-cadherin expression and boundary formation in developing forebrain. Development 124, 3765-3777.

Thakurela, S., Tiwari, N., Schick, S., Garding, A., Ivanek, R., Berninger, B., and Tiwari, V.K. (2016). Mapping gene regulatory circuitry of Pax6 during neurogenesis. Cell Discov 2, 15045.

Tuoc, T.C., Boretius, S., Sansom, S.N., Pitulescu, M.E., Frahm, J., Livesey, F.J., and Stoykova, A. (2013). Chromatin Regulation by BAF170 Controls Cerebral Cortical Size and Thickness. Developmental Cell 25, 256-269.

Tuoc, T.C., Radyushkin, K., Tonchev, A.B., Pinon, M.C., Ashery-Padan, R., Molnar, Z., Davidoff, M.S., and Stoykova, A. (2009). Selective cortical layering abnormalities and behavioral deficits in cortex-specific Pax6 knock-out mice. J Neurosci 29, 8335-8349.

Tuoc, T.C., and Stoykova, A. (2008). Trim11 modulates the function of neurogenic transcription factor Pax6 through ubiquitin-proteosome system. Genes Dev 22, 1972-1986.

van Bokhoven, H., and Kramer, J.M. (2010). Disruption of the epigenetic code: an emerging mechanism in mental retardation. Neurobiol Dis 39, 3-12.

Wang, X., Tsai, J.W., LaMonica, B., and Kriegstein, A.R. (2011). A new subtype of progenitor cell in the mouse embryonic neocortex. Nat Neurosci 14, 555-561.

Wen, S., Li, H., and Liu, J. (2009). Epigenetic background of neuronal fate determination. Prog Neurobiol 87, 98-117.

Wong, F.K., Fei, J.F., Mora-Bermudez, F., Taverna, E., Haffner, C., Fu, J., Anastassiadis, K., Stewart, A.F., and Huttner, W.B. (2015). Sustained Pax6 Expression Generates Primate-like Basal Radial Glia in Developing Mouse Neocortex. PLoS Biol 13, e1002217.

Xie, Q., Yang, Y., Huang, J., Ninkovic, J., Walcher, T., Wolf, L., Vitenzon, A., Zheng, D., Gotz, M., Beebe, D.C., et al. (2013). Pax6 interactions with chromatin and identification of its novel direct target genes in lens and forebrain. PLoS One 8, e54507.

Zhuo, L., Theis, M., Alvarez-Maya, I., Brenner, M., Willecke, K., and Messing, A. (2001). hGFAP-cre transgenic mice for manipulation of glial and neuronal function in vivo. Genesis 31, 85-94.

Acknowledgements

Scientific research is increasingly becoming a team effort and without the contribution of others, the results achieved through this thesis would have not been possible.

First and foremost, I would like to express my deep gratitude to Dr. Tran Tuoc, my supervisor and Prof. Jochen F. Staiger, head of the Institute of Neuroanatomy at the University Medical Center, for giving me the opportunity to conduct doctoral studies at the Institute. I feel sincerely grateful for the unrelenting support and supervision provided by them and the patience and belief that they had in me.

Special thanks to Dr. Tran Tuoc for providing me with a constant supply of animals/reagents, plenty of helpful advice, and constructive criticism. I was lucky to have excellent technical support from Linh Pham for histological techniques, genotyping and *in utero* electroporation. Many thanks to Dr. Robin Wagener and Dr. Alvar Prönneke for their help with microscopy and image processing.

I also want to thank Kamila Kiszka and Nieves Mingo Moreno for many fruitful discussions and the great time we had together, that really helped overcome the burdens of PhD. I wish to also thank all my colleagues for making the lab such a lovely place to work at.

I am grateful for the effort of Prof. Klaus-Armin Nave and Prof. Andre Fischer, members of my thesis committee, in providing different perspectives and enriching discussions that helped in shaping the project.

My sincere gratitude to Prof. Michael Hoerner and Sandra Drube from the IMPRS Neurosciences program. Since the moment I was admitted to the program, the excellent support and guidance provided by them helped me progress in my MS/PhD studies.

Last but definitely not least, I want to express the bliss of being unconditionally loved and supported in all my endeavors by my dear Mother, family and friends.

Thank you!